14. Econometric forecasting of climate change

Jennifer L. Castle, David F. Hendry and J. Isaac Miller

1. INTRODUCTION

This chapter will explain the basics of how the climate system functions; why climate change is occurring; how econometricians forecast in general and in the climate context; and how that compares with the way climate scientists think about uncertainty and make projections about future climate outcomes. Human behavior is the key determinant of climate change, particularly from burning fossil fuels like coal, oil and natural gas, and agriculture that release greenhouse gas emissions (GHGs) such as carbon dioxide (CO_2), nitrous oxide (N_2O) and methane (CH_4), which cumulate in the atmosphere and reflect back radiation. Macroeconometricians are practiced at modeling aggregate human economic behavior which is non-stationary from evolving trends and breaks deriving from many sources including pandemics, wars, technical progress, financial innovation, demography, and economic policy regimes. Many of these have impacts on the climate, so climate data is also non-stationary, and in turn feeds back on economic outcomes. The feedback is experienced acutely through events associated with extreme heat, such as mortality-threatening heat domes, events associated with anomalously high precipitation, such as inland floods from 'rivers in the sky' (see Lavers et al., 2018), coastal flooding from sea level rises (see Vitousek et al., 2017), and tropical cyclones (see Martinez, 2020; Bloemendaal et al., 2022), or events associated with anomalously low precipitation, such as droughts (see Trenberth et al., 2014) and wild fires.

Figure 14.1 shows some of these climate changes, starting with the huge increase in atmospheric CO_2 over the last 250 years from the Industrial Revolution onward, compared to variations over 800,000 years of eight ice ages coming and going (panel (a)). As a result, the planet has warmed, with the Arctic warming much faster (panel (b)) as melting sea ice reduces the reflectivity of sunlight and increases the heat absorption of the Arctic Ocean: see for example, Diebold and Rudebusch (2022), and as moisture assists in transporting heat from incoming radiation poleward: see section 3. The global increases in ocean heat content have extended down to 2000 meters (panel (c)), accompanied by a rise of more than 10 inches in sea level (panel (d)). Importantly, these changes have themselves been increasing, though not at constant rates, shown by the steepening trend lines fitted to each third of the data sample. Panel (d) illustrates how badly wrong a trend-based forecast made in 1925 would have been.

Forecasting the jump in CO_2 from 1760 would have required a forecast of economies continuing to be dependent on coal then oil and gas, ignoring the knowledge by 1900 that increased CO_2 would cause a warming climate (Foote, 1856; Arrhenius, 1896) that could be prevented by discoveries about generating electricity and the inventions of solar cells, wind turbines and electric vehicles with rechargeable batteries (Castle and Hendry, 2022, provide a brief history).

The success of econometric model-based forecasts depends upon (see Hendry, 1997): (a) there are regularities in the system being modeled; (b) those regularities are informative about

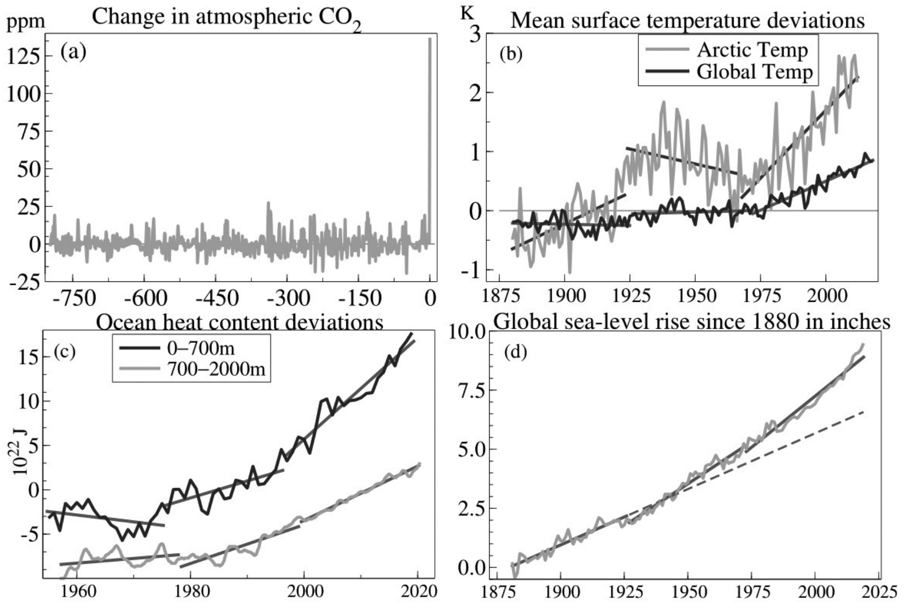

Figure 14.1 (a) Thousand-year changes of ±25 parts per million (ppm) in atmospheric CO_2 over 800,000 years of eight ice ages coming and going, then the last 250 years of +140ppm CO_2 where 1ppm = 7800 billion kg of CO_2; (b) annual global and Arctic mean surface temperature deviations in degrees K since 1880; (c) ocean heat content deviations to 700 and 2000 meters in 10^{22} Joules since 1960; (d) global sea level rise since 1880 in inches. Panels (b)–(d) show trend lines fitted to each third of the data sample to highlight changes

the future; (c) the estimated model captures the regularities; yet: (d) excludes irregularities that might swamp regularities. While there are important regularities in both climate and macroeconomic data, and many of those that are informative about the future are embodied in empirical systems, sudden unanticipated changes are not rare and can be large, leading to forecast failure. Recent examples with substantial impacts on climate-related economic variables include the 'Financial Crisis', Sars-Cov-2 pandemic and Russia's invasion of Ukraine (see Castle et al., 2021a, 2021b, for principles of forecasting applicable to non-stationary processes and model selection when forecasting).

Figure 14.2 focuses on more recent changes in CO_2. Panel (a) records monthly atmospheric CO_2 levels measured at Mauna Loa in parts per million (ppm) compared to an overall linear trend. This highlights that increases are increasing, shown in panel (b), despite the agreements

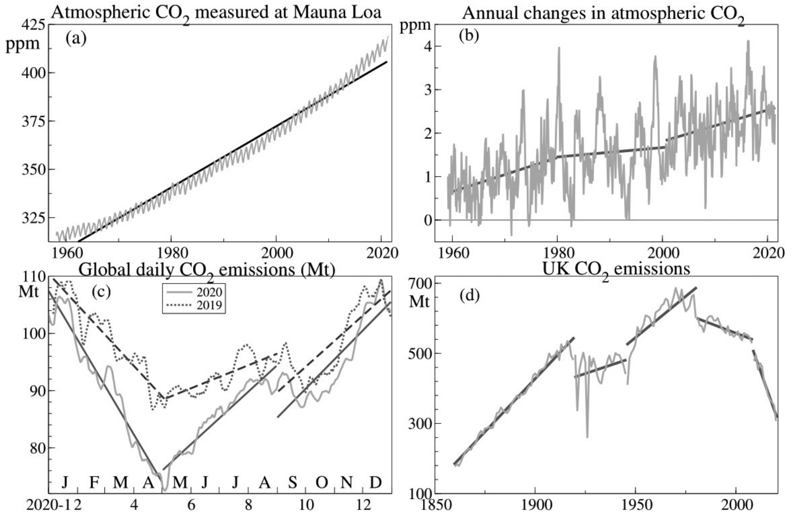

Figure 14.2 *(a) Monthly atmospheric CO_2 levels measured at Mauna Loa in ppm; (b) annual changes in atmospheric CO_2 in ppm; (c) reductions in CO_2 emissions in millions of tonnes (Mt) during 2020 from the SARS-Cov-2 pandemic compared to 2019 (source: Carbon Monitor); (d) UK CO_2 emissions in Mt per annum since 1860. Trends added to highlight changes*

at COP21 in Paris. Even the drastic lockdowns during 2020 from the SARS-Cov-2 pandemic barely dented emissions, reported in panel (c), which are in millions of tonnes (Mt) so are tiny compared to 4ppm. However, the UK territorial CO_2 emissions in panel (d) have fallen steeply this century having risen till 1980 after some violent fluctuations during the interwar years.

A common feature of all these graphs is non-constant change – changes keep changing, sometimes accelerating, sometimes slowing and occasionally dropping (see Ericsson et al., 2022, for a discussion and application to changing precipitation in Mauritania). This makes forecasting difficult as changes in the change are hard to anticipate. A break during a forecast interval will later become a break in-sample so will contaminate estimation of the parameters of econometric models unless properly handled, an issue addressed in section 4.

The structure of the chapter is as follows. Section 2 explains the climate science background, dependent on both the physical properties of the climate system and human behavior. Next, section 3 discusses the links between econometric and climate models and how climate scientists think about uncertainty and make their projections. Then section 4 describes how forecasts can go awry when there are shifting distributions and explains how modeling distributional shifts in-sample is critical for the production of long-run climate forecasts. Given those backgrounds, section 5 provides an example of forecasting climate variables 20 years ahead. Section 6 concludes. A short appendix includes data sources in Table 14A.1 and a rough calculation of the transient climate response entailed by our forecasts. All empirical analysis is conducted in OxMetrics version 9, and PcGive version 16.[1]

2. CLIMATE SCIENCE

The climate is determined by a complex interaction between the atmosphere, oceans and land, influenced by both natural forces (solar radiation, seasons, plate tectonics, volcanic eruptions, El Niño etc.) and anthropogenic factors (burning fossil fuels, land use for agriculture and forestry, dams to store water etc.) as well as the consequences of their interactions (reduced albedo from melting Arctic ice and other factors, aerosol pollution, changes in rainfall and cloud cover, wild fires, coastal erosion etc.). Emissions of GHGs from natural and anthropogenic sources cumulate in the atmosphere and re-radiate energy from the sun back to the planet, hence the label greenhouse gases.

Greenhouse gases have been increasing rapidly, especially CO_2, nitrous oxide N_2O, and methane CH_4 (see Cheng and Redfern, 2022), which have different impacts and residence times in the atmosphere making the so-called *recalcitrant component* of global warming (Held et al., 2010). Tian et al. (2020) conclude that recent growth in N_2O emissions exceeds some of the highest projected emission scenarios. Atmospheric CH_4 has been increasing from natural gas leaks, tundra melting, animal husbandry, and partly because of the large increase in wildfires which not only release CO_2 but also carbon monoxide that nullifies the hydroxl free radicals (OH) that help remove both CH_4 and pathogens. The latest Intergovernmental Panel on Climate Change (IPCC) report notes that CH_4 is responsible for about one-third of the 1.5°C of global warming, offset in part by sulfur dioxide emissions cooling around 0.5°C, so total warming is now about 1°C, with **half** due to CO_2. The pandemic lockdowns reduced GHG emissions but atmospheric concentrations still increased. Thus, just controlling GDP growth is not likely to get society to climate neutrality. Because of the large and recalcitrant (persistent) effect of CO_2 on warming, many studies focus exclusively on CO_2 emissions or concentrations as a proxy for all anthropogenic activity. However, all GHGs, including chlorofluorocarbons (CFCs), hydroCFCs, Hydrofluorocarbons (HFCs) and sulfur hexafluoride (SF_6) contribute to radiative forcing so the Earth receives more incoming energy from sunlight than it radiates back to space.

A *climate forcing*, or simply *forcing*, is defined by Hansen et al. (2017) as an imposed change in Earth's energy balance. *Total radiative forcing* is the sum of all forcings, whether natural or anthropogenic. The IPCC (2014a, Table 8.6) estimates the contributions of forcings to be within the intervals $(2.54, 3.12)$ W/m^2 (watts per square meter) for well mixed greenhouse gases, as well as providing estimates for other atmospheric layers, surface albedo due to black carbon and contrails. The sum of these with less well-understood effects of interactions of aerosols and contrails with clouds constitute total radiative forcing from anthropogenic sources.

[1] https://www.doornik.com/.

Solar irradiance (i.e., surface power density) and stratospheric aerosols from volcanic eruptions make up natural forcings. However, not all natural changes in the Earth's energy balance are forcings. Imbalances that are endogenous to the Earth system are *natural variability*, such as semi-periodic cycles like the El Niño Southern Oscillation, the Atlantic Multidecadal Oscillation, and the Pacific Decadal Oscillation. Changes in temperatures from these cycles have magnitudes large enough to *temporarily* offset anthropogenic forcing and cause apparent hiatuses (Kosaka and Xie, 2013) so may confound policy analysis (Miller and Nam, 2020).

The overall climatic outcome depends on both physical properties (energy balance etc.) and human behavior, so like macroeconomic data, most climate time series are non-stationary, exhibiting inertia, stochastic trends and distributional shifts from changing means and variances over time. Importantly, merely forecasting change is insufficient as many features of climate change depend on the levels of variables like atmospheric CO_2, which requires cumulating changes to levels when changes are forecast. Reasonably accurate forecasts of changes may cumulate to poor forecasts of levels: if an average growth rate of 2% per annum is forecast by 1.6% per annum, after five years the level is underpredicted by 2%. An example of this issue is illustrated in Figure 14.3 where small changes in the growth rate (panel (a)) cumulate to large changes in the level (panel (b)) which are hard to detect when forecasting the change.

2.1 Role of the Oceans and Sea Level Rises

Most of the excess energy stored in the climate system is taken up by the oceans leading to thermal expansion and sea level rise, which is 'baked in' by slow adjustment to past temperatures (Jackson et al., 2018). Thus forecasts of future serious coastal flooding (see Vousdoukas et al., 2018) are reliable, although outcomes will differ across Representative Concentration Pathways (RCPs) and would be worse if West Antarctic & Greenland ice masses melted much faster (Jackson et al., 2021). Re-measures of high-tide coastal heights have tripled estimates of global vulnerability to sea level rise and coastal flooding (Kulp and Strauss, 2019) emphasizing the need for accurate data. Jevrejeva et al. (2020) estimate the contribution from thermal expansion to sea level rise using the simulations of global mean thermosteric sea level (GMTSL) from 15 available models in the Coupled Model Intercomparison Project Phase 6 (CMIP6). They calculate GMTSL rises of 18.8 cm and 26.8 cm to 2100, relative to 2014 for Shared Socioeconomic Pathways SSP245 and SSP585 scenarios, approximately RCP4.5 and RCP8.5 respectively.

Storm surge heights are very dependent on local conditions – and the resulting economic damages more so (Martinez, 2020; Jevrejeva et al., 2018). Sea level rise will intensify coastal flood risk by changing the amplitude and occurrence of storm surges, called the return period as shown in Figure 14.4. A return period is the estimated time between events of a similar size. For example, the return period of a storm surge that reaches one meter above sea level might be 100 years. The chance that this flood level occurs in any one year is therefore approximately 1/100, or 1%.

Jackson and Hendry (2018) show how dramatically flood level return periods can shift depending on their non-linearity. If a given magnitude of storm surge return period remained the same in the future, then a rise in the sea level would shift the levels of each return period up so it would occur more often. Moreover, each return period magnitude would have increased by the

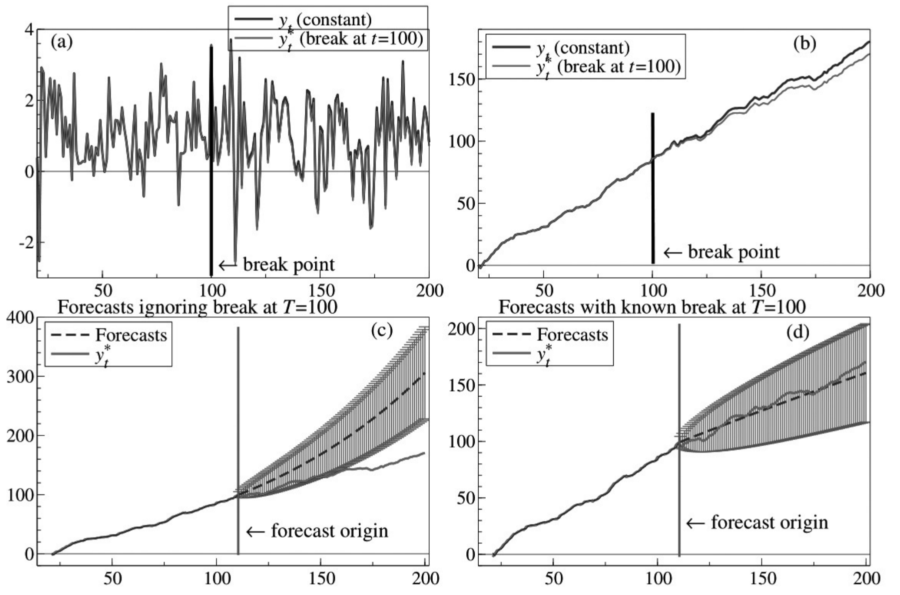

Figure 14.3 *(a) Data-generating process is a random walk superimposed by a process with a break in trend growth at* $t = 100$*; (b) same processes in levels; (c) 90 dynamic forecasts from* $T = 110$ *with* $\pm 2\hat{\sigma}_f$*; (d) forecasts assuming a known break at* $t = 100$ *with* $\pm 2\hat{\sigma}_f$

amount of sea level rise. For cities like London, long-term storm-surge records are fairly accurate, as are forecasts of sea level rises, so predictions of a dramatic reduction in periods between serious flooding must be taken seriously, even if the exact dates are unpredictable (see Vitousek et al., 2017). While forecasting the relevant 'local' sea level rise would be the main contributor to forecasting return periods and their magnitudes, contemporaneous wind speeds also matter but are harder to forecast. Return periods apply to many weather phenomena including inland floods, droughts, heat waves, and max day and night-time temperatures.

Using the average local sea level projection by 2100 under business-as-usual (RCP8.5) for London (Jackson and Jevrejeva, 2016), the present-day 1-in-500 year flood level has shifted to a future 1-in-20 year flood level, which is on the order of 25 times more likely to occur. Further, the 1-in-500 year flood level would increase from 200 cm to 274 cm, so like many other cities worldwide, London needs to protect itself from more frequent floods of a larger size.

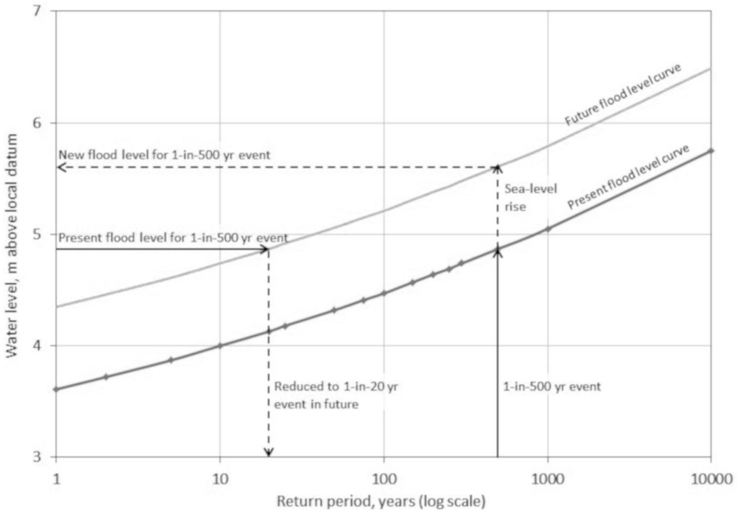

Note: Projected flood levels are calculated by the addition of the projected sea level rise (74 cm, under RCP8.5 scenario).
Source: (Sheerness tide gauge, Environment Agency 2011), Coastal flood boundary conditions for UK mainland and islands. https://www.gov.uk/government/collections/thames-estuary-2100-te2100.

Figure 14.4 Present-day and projected flood level return periods for London

3. CLIMATE MODEL FORECASTING

Strictly speaking, much of what we think of as 'climate forecasts' are not forecasts. At best, they are *conditional* forecasts with certain anthropogenic scenarios in mind. In fact, climate scientists do not use this terminology at all but refer to such projections as *simulations* of an underlying physical climate model.

Physical climate models rely at their core on energy budgeting to adhere to the first law of thermodynamics. While that principle has not changed, the complexity of the models has grown with the computing power available to well-financed research teams. Early models can be estimated and used to forecast global aggregates in seconds on a laptop. State-of-the-art models require weeks or months to run using state-of-the-art computing resources.

Energy balance climate models, or simply *energy balance models* (EBMs), constitute the first generation of physical climate models. A so-called zero-dimensional EBM equates global temperature change to a proportion of the difference between incoming solar energy and outgoing energy radiated by the Earth. The late 1960s saw the independent development of one-dimensional EBMs by Budyko (1969) in the Soviet Union and Sellers (1969) in the United States, which explicitly model horizontal latitudinal net heat transport. One-dimensional EBMs were followed in the 1970s by one-and-a-half-dimensional and then two-dimensional EBMs (Sellers, 1976), which allow horizontal net heat transport to be driven by more complex forces so that temperatures may vary over both latitude and longitude.

Important contributions to the mathematical formulations of EBMs were made by Held and Suarez (1974), North (1975), North and Cahalan (1981), North et al. (1981), and North et al. (1983), among others. Interestingly, these models either lack anthropogenic components entirely or else have a weakly stationary component (c.f. North et al., 1981). Although such stochastic forcings may be interpretable in retrospect as anthropogenic, it would be hard to argue for stationarity of the anthropogenic forcing given the data of the four decades that have transpired since this work was published, even though Davidson et al. (2016) find evidence of stationarity over the much longer time span of the paleoclimatic record.

Some of the more recent literature has focused on improving our understanding of low-dimensional EBMs. For example, Langen and Alexeev (2007), Merlis and Henry (2018), and Siler et al. (2018) improve on the net heat transport function in a simple one-dimensional model by allowing the transportation of moisture to better model *polar amplifications* (PA), in which poleward temperatures – worryingly near Greenland ice sheets, Antarctic ice sheets, and Siberian permafrost – increase faster than those near the Equator. Aside from the possibility of triggering tipping points in these regions, Francis and Vavrus (2012) link PA to extreme weather at mid-latitudes and Brock and Xepapadeas (2017) link a failure to account for PA to suboptimal climate policy, both of which have obvious economic impacts.

Implied relationships in spatially aggregated or disaggregated data from low-dimensional EBMs are explored by Matthews et al. (2009), Leduc et al. (2016), Pierre Perron and his coauthors (Estrada et al., 2013a, Estrada et al., 2013b; Estrada and Perron, 2014), and Robert Kaufmann and his coauthors (Stern and Kaufmann, 2000, 2014; Kaufmann et al., 2006a, 2006b, 2010, 2011, 2013, and Chang et al., 2020) among many others.

3.1 Global Climate Models

State-of-the-art climate forecasts are not made by energy balance models, but by a class of models known as atmospheric-ocean general circulation models, more simply as general circulation models, or more recently as *global climate models* (GCMs). Using available computing power, GCMs push the physical representations of climate phenomena to finer and finer levels of spatial and temporal disaggregation. To give readers an idea of the scale, one of the main obstacles of such systems today is to model the physics underlying the interactions of aerosols with clouds, which is not only difficult to model but also difficult to understand (IPCC, 2014b). The complexity of GCMs poses a serious barrier to entry for most researchers, which has forced modeling efforts in several directions.

One such direction is consensus within the scientific community to examine certain common scenarios. Common scenarios facilitate model comparisons: the use of models for common purposes is a core principle of the CMIP. The first generation of scenario research culminated in the Special Report on Emissions Scenarios (SRES), which produced scenarios used by the IPCC from 2000. These were replaced by the RCPs, which focus on the concentrations of greenhouse and other gases rather than on their emissions. Moss et al. (2010) trace a history of the use of scenarios in climate science up to this point. Most prominent and most extreme among the RCPs is RCP8.5, (Riahi et al., 2011), long considered to be a business-as-usual scenario, but now considered by many to be too extreme following criticisms by Hausfather and Peters (2020) and others. The current generation of SSP pathways (Riahi et al., 2017) expand on RCPs by allowing for alternative scenarios in economic and population growth.

Why is consensus around a relatively small number of scenarios important? Weather and climate forecasts face uncertainty around the initial conditions of their forecasts. Slight mistakes in the measured state of the atmosphere can grow rapidly over time leading to large errors in the future. Ensemble forecasts are therefore used, where a given computer model is run a number of times from slightly different initial conditions to estimate the uncertainty around the central forecast: see Palmer (2006, 2022). The physical climate system is evolving due to GHGs whose future path is highly uncertain, being dependent on human use of fossil fuels and agricultural practices. Consequently, climate models report projections of future outcomes conditional on concentration pathways like RCP8.5. Uncertainties are focused around these, rather than unconditional outcomes.

Not only does a consensus around such scenarios provide a scientific basis for discourse, it also allows researchers to evaluate uncertainty using multi-model ensembles. Santer et al. (1990) proposed using variation in output over such multi-model ensembles as a proxy for inter-model uncertainty, in what we might call a meta-analysis. Studies using multi-model ensembles can produce some rather striking graphical representations, such as those generated by Dietz et al (2021) Figure 1, common scenario, or the different scenarios in Figure 1 of Fawcett et al. (2015). Aggregating such outputs for the purpose of (conditional) forecasting is akin to the practice of pooling or aggregating forecasts familiar to economists (Hendry and Clements, 2004). Santer et al. (1990) warn of the risks of combining models for this purpose, and this sentiment has been echoed by a number of authors who have improved on the basic methodology to assess uncertainty, such as Tebaldi and Knutti (2007), Knutti et al. (2010), and Rasmussen et al. (2016).

With some notable exceptions, such as Bayesian model averaging, economists and statisticians often frame model uncertainty in terms of a known model with unknown coefficients and some sort of error specification to allow for unobserved determinants of the data we wish to explain. The uncertainty underlying a meta-analysis based on a common set of input data lies in different models and different initial conditions used to simulate the same model. In this sense, the intervals implied by the figures in Dietz et al. (2021) and Fawcett et al. (2015) have quite different interpretations than those of fan charts published by central banks, for example.

3.2 Statistical Emulation of GCM Output

An alternative to combining model output to assess future uncertainty is *statistical emulation* of GCM output, like that conducted by Castruccio et al. (2014) or Miftakhova et al. (2020), which allow for the use of classical statistical methods such as the bootstrap (Poppick et al., 2017). Castruccio et al. (2014) construct spatially disaggregated models simply by mapping spatially disaggregated temperatures to a common spatially aggregated anthropogenic series of climate forcings, while the more traditional method of *pattern scaling* maps spatially disaggregated temperatures to global mean temperatures, along the lines of Santer et al. (1990), Lopez et al. (2014), and Tebaldi and Knutti (2018).

Statistical emulation allows not only for rapid approximation of GCM output in response to a well-known scenario for emissions or concentrations of greenhouse and other gases, such as RCP8.5 or SSP2-Baseline, it also allows for the possibility to leverage the relationships between climate variables and such a pathway to approximate the climate response to scenarios with intermediate emissions or concentrations pathways. Huntingford et al. (2017) approximate pathways using parsimonious statistical models. Miller and Brock (2024) go a step further by locally weighting the parameters of a family of parsimonious statistical models that approximate hundreds of peer-reviewed AR5 pathways. Novel pathways, called quasi-representative concentration pathways, can be created that mimic pathways resulting in similar GHG concentrations in a target year, often 2100, but that were produced by much more complicated models.

On a range of complexity between simple reduced-form statistical models and techniques like the emulation model of Castruccio et al. (2014) or the pattern scaling technique of Santer et al. (1990), for example, and fully-fledged GCMs, lie Earth system models of intermediate complexity (EMICs), such as the MIT Earth systems model of Sokolov et al. (2018) and Monier et al. (2018) and the MAGICC models of Wigley and Raper (1987) and Meinshausen et al. (2011). As Claussen et al. (2002) point out, the degree of complexity of such models aims to capture the most important features of GCMs, yet can be run quickly enough to assess uncertainty through multiple runs and to produce results on a policy-relevant time scale.

3.3 Integrated Assessment Models

Integrated assessment models (IAMs), dating back to William Nordhaus's 1993 contribution of the DICE (dynamic integrated climate-economy) model, use the scenarios discussed above to price carbon and climate change mitigation more generally (see Azar and Sterner, 1996, and Kaufmann, 1997, for critiques of DICE). To paraphrase Nordhaus (2013), IAMs begin with human activity in the form of emissions and end with human activity in the form of economic damages from anthropogenic climate change. The complexity of IAMs has grown over time, though not as much as GCMs. Coupling a modern IAM with an EMIC by Monier et al. (2018) allows for a model-consistent framework to assess economic and climate scenarios and policy.

As Santer et al. (1990) note, climate impact studies require data that are sectorally, spatially, and temporally disaggregated. Yet, such observational data effectively did not exist until recently. Thus, many empirical climate studies rely on model outputs as data rather than on observational data. Neither type of data come without risk. Econometricians are used to thinking about measurement error in observational data, such as those that lead to revisions in GDP. And like some long-run economic data such as unemployment (see Boyer and Hatton, 2002), the whole time span of observational climate data may be subject to revision when new methods are found to address known measurement errors. Moreover, in spite of the availability of satellite and other high-resolution data sources, missing data are pervasive in the historical record. Model output data can be obtained at virtually any resolution but cannot be utilized directly and must be *bias-corrected* using the historical record (e.g., Ivanov et al., 2018).

3.4 Direct Links between Climate Models and Econometric Systems

While most climate econometric time-series analyses do not strictly impose energy balance properties, allowing for measurement error, etc., they seek to be consistent with the conservation of energy required by principles (first law) of thermodynamics.

Following the application of cointegration methods to climate by Stern and Kaufmann (2000), Kaufmann and Stern (2002), Schmith et al. (2012), and Kaufmann et al. (2013), Pretis (2020) shows an energy-balance model of global temperature, ocean heat content and radiative forcing is equivalent to a cointegrated system that can be estimated from discrete-time data. The estimated parameters can quantify uncertainties in IAMs of the economic impacts of climate change. Accounting for structural breaks from volcanic eruptions highlights large parameter uncertainties and shows that previous empirical estimates of the temperature response to increased CO_2 concentrations may be misleadingly low.

Bruns et al. (2020) model the ocean surface temperature and radiative forcing as multicointegrated processes (see Granger and Lee, 1990). Specifically, both series are I(1) and cointegrate along the lines of extant literature, while the accumulation of the disequilibrium error from this cointegrating relationship, which represents the change in the Earth's heat content stored in the ocean, also cointegrates with ocean surface temperature. Ocean surface temperature therefore shares a long-run stochastic trend with radiative forcing and with the net deviations of temperature from its long-run equilibrium with that forcing. This second cointegrating relationship allows for persistent deviations of surface temperatures away from equilibrium as the oceans absorb excess energy from radiative forcing, so that the surface temperature adjusts more slowly than it otherwise would. Indeed, they find that the rate of adjustment to equilibrium is realistically slow – that is, if atmospheric CO_2 doubled then Earth would eventually be 2.8°C warmer, noting CO_2 has risen about 50% from 280ppm: see Figure 14.1(a).

Brock and Miller (2023) show that moist energy-balance models, which allow for horizontal (latitudinal) net heat transport by way of moisture like those of Langen and Alexeev (2007) and Merlis and Henry (2018) mentioned above are equivalent to a cointegrated system. Although the system is nonlinear in the structural parameters, they can be identified to test for PA and conduct impulse response functions and forecasts that realistically allow for more warming near the poles than near the equator.

4. IMPLICATIONS OF SHIFTING DISTRIBUTIONS FOR FORECASTING

The previous section highlights the complexity of GCM forecasting, so in this section we discuss the use of statistical forecasting methods for prediction of climate data. The forecast horizon is typically much longer than traditional economic forecasting, although there has been recent interest in statistical long-horizon forecasts, see for example Müller and Watson (2016), Baek (2019) and Lunsford and West (2021). For longer horizon forecasts, non-stationarity plays a key role. Breaks in trend over the forecast period may be inherently unpredictable, depending on both exogenous shocks and distant policy changes, but conditional forecasts based on assumptions regarding future policy and events are feasible. A key feature of forecasting models is whether they are closed, so all their variables are modeled, or open, so some variables are unmodeled and conditional forecasts are made (see Hendry and Mizon, 2012). Reporting a number of possible future scenarios (e.g., for different RCPs) is common in the climate literature, albeit that at least all but one must be wrong in the event (see Hendry and Pretis, 2023), but less common with statistical models.

As discussed by Pretis (2021), exogeneity of the conditioning variables plays a key role in the econometric analysis of climate. He views the field of climate econometrics as being split between studies that take climate as given and assess the economic impacts or damages from climate change and studies that take anthropogenic scenarios as given and assess the impact of the resulting forcing on the climate system. Many of the empirical studies referenced in this chapter fall in the second group with the notable exception of integrated assessment models along the lines of DICE, which allow for simple feedbacks between the climate system and the economic system. Pretis (2021) argues that exogeneity may be a plausible assumption if so-called tipping points are not a concern on the climate side or if policy invariance is plausible on the economic side. In other words, anthropogenic forcing may be viewed as exogenous with respect to climate when the resulting climate change is not large enough to trigger substantial nonlinearities in the climate system, such as the release of methane from melting permafrost, and climate may be viewed as exogenous with respect to economic impacts when climate policy is invariant with respect to those impacts.

The key role of invariance of model parameters to policy interventions and environmental changes (Engle and Hendry, 1993; Castle et al., 2017) also matters, and is intimately linked to exogeneity. Engle, Hendry and Richard (1983) define invariance as parameters which remain constant and can be estimated without difficulty even when interventions occur over the sample period. Invariance is not known *a priori* but can be tested using saturation tests for location shifts in the marginal model which are then tested for significance in the conditional model, see Hendry and Pretis (2023) who discuss how a lack of invariance has implications for scenario forecasts. Super-exogeneity combines exogeneity with parameter invariance, which if satisfied, enables the model to infer implications about the climate from policy interventions.

Long-horizon forecasts depend critically on the trend that is extrapolated from the forecast origin. This is one of the key differences between climate forecasts from physical models and those from statistical models: physical model forecasts vary the initial conditions of the otherwise deterministic systems to gauge the degree of uncertainty in the long-run projections whereas statistical models are inherently stochastic and vary the model specification and stochastic disturbance term but often take the initial conditions as known.

The importance of an accurate estimate of the underlying trend for long-range forecasts is highlighted in Figure 14.4. The data-generating process is a random walk with drift at 1% p.a., but its growth rate shifts down by 0.1% at $t = 100$, which is almost indiscernible to the eye (panel (a)), and is only detected in levels after 10 observations (which we assume to be years, panel (b)). If the break in trend is unmodeled, the forecasts from a forecast origin at $T = 110$ show a diverging trend and increasing forecast errors over the 90 years (panel (c)), but panel (d) demonstrates that forecasts can be accurate over long horizons if the trend break is known and correctly modeled. There were 10 observations prior to the forecast origin to detect the trend break; typically small changes in growth rates are hard to detect but have a big impact in the long-run. Other aspects of model specification are of secondary importance compared to the trend when forecasting 50 or 100 years into the future.

4.1 Modeling Distributional Shifts in Climate Data

Climate change is not happening at a constant rate, so forecasters need to address how to handle non-stationarities caused by shifts and breaks as well as smoothly-varying deterministic functions. As Figure 14.1(b) showed and section 3 discussed, the Arctic is warming much faster than the rest of the planet, and as Diebold and Rudebusch (2022) demonstrate, Arctic ice cover is disappearing at increasingly rapid rates. Figures 14.1(c) and (d) show accelerating ocean heat content and global sea level rises. Although those graphs plot deterministic trends, those are descriptive, not components of their data-generating processes, which reflect responses to increasing atmospheric levels of greenhouse gases, and will change when those do. Thus, changes in dynamics need to be taken into account as well as location shifts, including events like the impacts of COVID-19 lockdowns on economic outcomes and in turn on greenhouse gas emissions.

There is an extensive literature that provides solutions to in-sample shifts, including selecting observations that exclude the break (see Pesaran and Timmermann, 2007; Pesaran et al., 2013); fitting to expanding or rolling windows (see Giacomini and Rossi, 2009; Inoue et al., 2017); testing for and conditioning on breaks (see Bai and Perron, 1998); applying model selection using break indicators (see Castle et al., 2023); and switching to predictors that are robust following shifts to avoid forecast failure (see e.g., Hendry, 2006; Castle et al., 2015a; Martinez et al., 2022). For unanticipated forecast period shifts, namely events that occur after forecasts are made, little can be done, like the sudden onset of COVID-19. Even when there are antecedents that might help predict a shift – perhaps from information going beyond the relevant discipline's information on 'regular forces', such as advance warning of an El Niño – difficulties remain as discussed by Castle et al. (2010, 2011).

We next outline indicator saturation methods applied to climate data. These techniques are particularly useful as they have power to detect trend breaks at or close to the forecast origin which is crucial for long-horizon climate forecasts. Subsection 4.3 tests for changes in the dynamics of the UK's CO_2 emissions following the policy changes.

4.2 Indicator Saturation Estimators and Their Use in Forecasting

Indicator saturation estimators (ISEs) are designed to detect outliers, shifts in mean, or shifts in trends (inter alia) at any point in the data sample without relying on knowledge of their number, signs, magnitudes or timing. The principle involves generating an indicator variable for every observation in the sample for adding to the set of regressors to search for their significance. These indicator variables could be impulse dummies, $I_j = 1$ for $t = j$ and zero otherwise $\forall j \in T$ (impulse indicator saturation: IIS, Hendry et al., 2008); step dummies, $S_j = 1_{t \leq j}$ and zero otherwise (step indicator saturation: SIS, Castle et al., 2015b); or trend breaks which are the cumulation of step indicators (trend indicator saturation: TIS, Castle et al., 2019). The trend breaks are designed to be zero in the forecast period:

$$\tau_2' = (-1, 0, \dots, 0), \dots, \tau_t' = (-t+1, -t+2, \dots, -1, 0 \dots 0), \dots, \tau_T' = (-T+1, \dots, -1, 0).$$

Adding all indicators to the model at once would result in a perfect fit, but using a tree search algorithm with expanding and contracting block searches allows every indicator to be investigated for possible significance, see Doornik (2009) for details of the search algorithm. Selection needs to be done at very tight significance levels to control the probability of retaining irrelevant indicators given their high dimensionality, particularly if impulses, steps and trends are searched jointly, denoted super-saturation (Ericsson, 2012). Extensions of multiplicative indicator saturation (MIS: Kitov and Tabor, 2015) where step indicators are interacted with conditioning regressors and multiplicative step indicator saturation (MSIS: Castle et al., 2023), which uses a two stage procedure to model breaks in dynamics by interacting retained step indicators with the lagged dependent variable, have been developed.

We illustrate saturation estimators for atmospheric global CO_2. Figure 14.5(a) shows an increasing trend since the 1950s, where the data over 1862–2018 contain an explosive root which has severe implications for the long-horizon forecasts. Instead we model the annual change in log CO_2 recorded in panel (b), which shows a trend from the 1950s onwards.[2] There was a change in both measurement and reporting frequency post-World War II which is evident from some interpolation in the earlier part of the sample as well as an increase in variance in the latter part of the sample. Pretis and Hendry (2013) discuss the problems of merging time series from different measurement systems pre and post Keeling (see e.g., Keeling et al., 1976, Sundquist and Keeling, 2009). Rather than excluding the earlier sample due to these measurement issues we can use saturation estimators to handle the measurement changes. The forecasts discussed in this section are naïve benchmarks based on extrapolating past trends and are used to illustrate the importance of trend estimates at the forecast origin. Section 5 develops a more substantive forecasting model.

To scale coefficients conveniently, we multiply Δco_2 by 100, denoted $\%\Delta co_2$ then assuming constant parameters over the period 1862–2018 we obtain:

$$\widehat{\%\Delta co_{2,t}} = -\underset{(0.017)}{0.019} + \underset{(0.06)}{0.60}\ \%\Delta co_{2,t-1} + \underset{(0.0003)}{0.0014}\ \tau$$
$$\hat{\sigma} = 0.1\ \mathsf{R}^2 = 0.75\ \mathsf{F}_{\mathsf{ar}}(2, 152) = 7.9^{**}\ \chi^2_{\mathsf{nd}}(2) = 23.4^{**}$$
$$\mathsf{F}_{\mathsf{arch}}(1, 155) = 6.7^{**}\ \mathsf{F}_{\mathsf{het}}(4, 152) = 7.3^{**}\ \mathsf{F}_{\mathsf{reset}}(2, 152) = 3.9^{**} \tag{1}$$

where τ is a full sample deterministic trend.[3] The model fails all diagnostics but has a positive deterministic trend. The resulting level forecasts of CO_2 after transforming from differences

[2] Lower case denotes logs.

[3] Coefficient standard errors are shown in parentheses, $\hat{\sigma}$ is the residual standard deviation, R^2 is the coefficient of determination and $\mathsf{R}^{2\dagger}$ is the coefficient of determination excluding impulse indicators, F_{ar} tests for residual autocorrelation (see Godfrey, 1978), $\chi^2_{\mathsf{nd}}(2)$ tests for

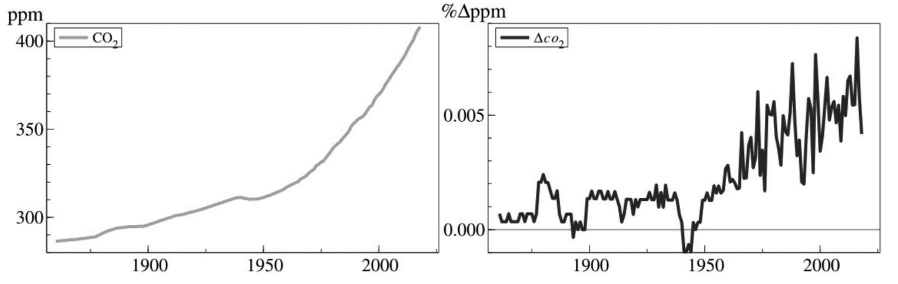

Figure 14.5 (a) Global atmospheric CO_2 in ppm; (b) the change in log CO_2 (Δco_2)

and logs are recorded in Figure 14.6 which predicts global levels of CO_2 above 680ppm by 2100. This is in line with the predictions from the White House Initiative on Climate Change that predicts that if the world continues on a 'business as usual' path, atmospheric CO_2 concentrations will be likely to exceed 700ppm by 2100.[4] However, we cannot be confident in the forecasts from this mis-specified model and the confidence intervals are not reflective of the degree of uncertainty in these predictions.

We next apply IIS+TIS at a selection significance level of $\alpha = 0.0001 = 0.01\%$, not selecting the lagged dependent variable, the constant and the trend, and switching off all diagnostics as the model is mis-specified. The resulting selected model over 1862–2018 is:

$$\begin{aligned}
\widehat{\%\Delta co_{2,t}} = &\underset{(0.06)}{0.48}\ \%\Delta co_{2,t-1} + \underset{(0.28)}{0.51} - \underset{(0.0019)}{0.0017}\ \tau + \underset{(0.07)}{0.26}\ I_{1966} + \underset{(0.07)}{0.32}\ I_{1973} \\
&+ \underset{(0.07)}{0.31}\ I_{1977} + \underset{(0.07)}{0.25}\ I_{1988} - \underset{(0.07)}{0.23}\ I_{1992} - \underset{(0.07)}{0.29}\ I_{1997} \\
&+ \underset{(0.07)}{0.37}\ I_{1998} - \underset{(0.07)}{0.21}\ I_{2000} + \underset{(0.07)}{0.32}\ I_{2016} - \underset{(0.001)}{0.006}\ \tau_{1966} + \underset{(0.0026)}{0.008}\ \tau_{1997}
\end{aligned}$$

$$\hat{\sigma} = 0.07\ \mathsf{R}^2 = 0.89\ \mathsf{R}^{2\dagger} = 0.77\ \mathsf{F}_{ar}(2, 141) = 3.6^{*}\ \chi^2_{nd}(2) = 4.0$$
$$\mathsf{F}_{arch}(1, 155) = 4.6^{*}\ \mathsf{F}_{het}(8, 139) = 5.5^{**}\ \mathsf{F}_{reset}(2, 141) = 11.4^{**} \quad (2)$$

where I_{xxxx} denotes an indicator for year *xxxx* and τ_{xxxx} denotes a trend that ends in year *xxxx*.

Although the model is still mis-specified, saturation picks up two trends and shows an increase in $\%\Delta co_2$ from the mid-1960s, which is then dampened in 1997 (the trend indicators

non-Normality (see Doornik and Hansen, 2008), F_{arch} tests for autoregressive conditional heteroscedasticity (see Engle, 1982), F_{het} tests for residual heteroskedasticity (see White, 1980) and F_{reset} tests nonlinearity (see Ramsey, 1969). One star indicates test significance at 5%, two at 1%.

4 https://clintonwhitehouse5.archives.gov/Initiatives/Climate/next100.html

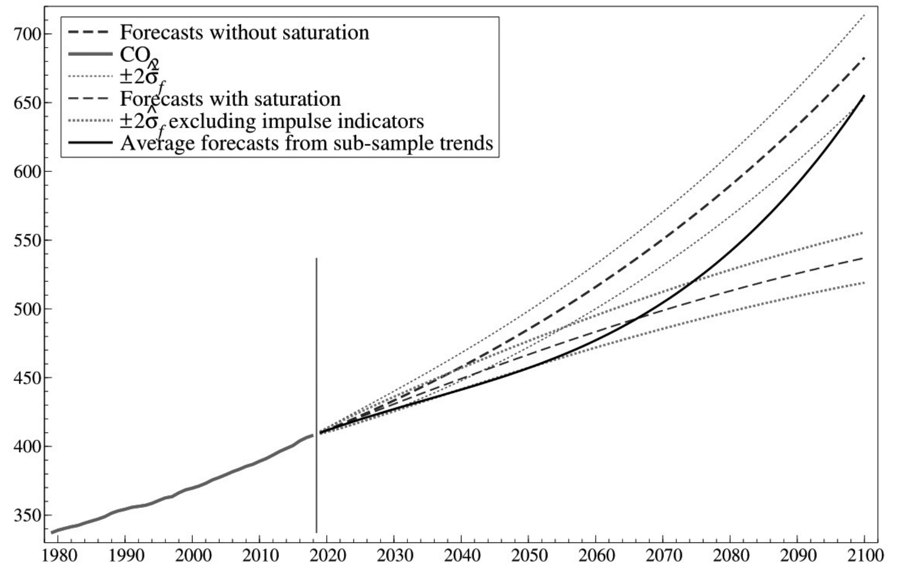

Figure 14.6 Dynamic forecasts for CO_2 from (1) in bold dashed (uncertainty bands in thin dotted), (2) in long-dashed (uncertainty bands in thick dotted) and the average forecasts across models in which a trend break is included between 2007 and 2016 in solid

are defined to be zero from the break onward, so the trend increases by 0.002 between 1966 and 1997 and then falls by 0.002 after 1997). This has a significant impact on the long-run forecasts as shown in Figure 14.6. The forecast standard errors are computed with the parameters from the selected model as fixed but excluding the impulse indicators which reduce the equation standard error. This predicts roughly 540ppm by 2100 which is equivalent to the predictions under RCP4.5, see Smith and Myers (2018).

The confidence bands for both models reflect the uncertainty associated with the specified model. To closer replicate the uncertainty over the initial conditions that climate scientists consider, we estimate the trend growth over the last $T - j, \dots, T$ years of the sample, where $j = 2, \dots, 12$ and then we average the resulting forecasts in levels, recorded by the solid line in Figure 14.6. Thus, uncertainty of the trend at the forecast origin plays a significant role in long-horizon forecasts and emphasizes the importance of break detection at or near the forecast origin, see Castle et al. (2023) which extends Clements and Hendry (1998) for single equations and Hendry and Mizon (2012) for a system with unmodeled explanatory variables.

4.3 Induced Impacts of Policy Changes on the UK's CO_2 Emissions

Equilibrium mean shifts can occur directly through changing intercepts or the means of conditioning variables, or be induced by shifts in dynamics that have non-zero means, see Castle et al. (2023). Here we test whether the three major policy intervention shifts detected by SIS in the United Kingdom's CO_2 emissions in Castle and Hendry (2022) (i.e., 1925, 1969 and 2010) were induced by changes to the dynamics. Using MSIS, we add the interactions of their step indicators with the lagged regressand to their empirical model of E_t (CO_2 emissions) on C_t (coal volumes in millions of tonnes, Mt), O_t (net oil usage in Mt) k_t (log of the capital stock), and g_t (log of real GDP), their lags and ISEs, estimated over 1861–2013. Selecting relevant variables by Autometrics at $\alpha = 0.01 = 1\%$ yielded a substitution of S_{2010} by its interaction with E_{t-1} (testing constancy over $2014-2017$)[5]

$$\begin{aligned}\widehat{E}_t = &\underset{(0.06)}{0.42}\, E_{t-1} - \underset{(13)}{47}\, I_{1921} - \underset{(10)}{80}\, \Delta I_{1926} + \underset{(6.9)}{50}\, \Delta I_{1947} + \underset{(9.8)}{29}\, I_{1996} \\ &+ \underset{(4.5)}{32}\, S_{1925} - \underset{(7.4)}{32}\, S_{1969} + \underset{(0.014)}{0.075}\, S_{2010}E_{t-1} - \underset{(85)}{147} + \underset{(0.12)}{1.90}\, C_t - \underset{(0.17)}{0.84}\, C_{t-1} \\ &+ \underset{(0.26)}{1.70}\, O_t - \underset{(0.28)}{0.99}\, O_{t-1} + \underset{(0.32)}{0.93}\, g_t - \underset{(0.32)}{1.07}\, g_{t-1} + \underset{(1.8)}{7.52}\, k_t - \underset{(1.8)}{6.9}\, k_{t-1}\end{aligned}$$

$$\begin{aligned}&\hat{\sigma} = 9.58 \;\; \mathsf{R}^2 = 0.995 \;\; \mathsf{F}_{\mathsf{ar}}(2,134) = 1.08 \;\; \mathsf{F}_{\mathsf{arch}}(1,151) = 3.32 \;\; \mathsf{F}_{\mathsf{het}}(21,124) = 0.67 \\ &\chi^2_{\mathsf{nd}}(2) = 4.28 \;\; \mathsf{F}_{\mathsf{reset}}(2,134) = 2.75 \;\; \mathsf{F}_{\mathsf{chow}}(4,136) = 1.28 \;\; \mathsf{F}_{\mathsf{nl}}(27,106) = 1.18 \qquad (3)\end{aligned}$$

The resulting cointegration relation was (noting that step indicators need to be led in its formulation as the equilibrium correction will enter the empirical model lagged one period):

$$\begin{aligned}\widetilde{E}_{LR,t} = &\underset{(0.07)}{1.75}\, C_t + \underset{(0.16)}{1.22}\, O_t + \underset{(0.24)}{1.03}\, k_t - \underset{(0.24)}{0.24}\, g_t + \underset{(6)}{55}\, S_{1924} - \underset{(12)}{55}\, S_{1968} \\ &+ \underset{(0.02)}{0.13}\, S_{2009}E_{t-1} - \underset{(142)}{253} \qquad (4)\end{aligned}$$

[5] $\mathsf{F}_{\mathsf{chow}}$ tests for parameter constancy (see Chow, 1960) and F_{nl} tests omitted non-linearity (see Castle and Hendry, 2010).

Reformulating as a differenced model with the additional impulse indicators previously found for 1912 and 1978 where $\tilde{Q}_t = E_t - \tilde{E}_{LR,t}$:

$$\widehat{\Delta E}_t = \underset{(0.10)}{1.87}\,\Delta C_t + \underset{(0.21)}{1.67}\,\Delta O_t + \underset{(1.09)}{7.22}\,\Delta k_t + \underset{(0.28)}{0.91}\,\Delta g_t - \underset{(0.05)}{0.57}\,\tilde{Q}_{t-1} + \underset{(2.09)}{2.30}$$
$$- \underset{(8.72)}{80.3}\,\Delta I_{1926} + \underset{(6.40)}{50.1}\,\Delta I_{1947} - \underset{(11.0)}{46.8}\,I_{1921} - \underset{(8.92)}{27.9}\,I_{1912}$$
$$+ \underset{(8.92)}{27.3}\,I_{1978} + \underset{(8.91)}{29.1}\,I_{1996}$$
$$\hat{\sigma} = 8.85 \;\; \mathsf{R}^2 = 0.94 \;\; \mathsf{F}_{\mathsf{ar}}(2, 138) = 0.42 \;\; \mathsf{F}_{\mathsf{arch}}(1, 150) = 0.56 \;\; \mathsf{F}_{\mathsf{het}}(14, 133) = 1.08$$
$$\chi^2_{\mathsf{nd}}(2) = 1.65 \;\; \mathsf{F}_{\mathsf{reset}}(2, 138) = 1.56 \;\; \mathsf{F}_{\mathsf{chow}}(4, 140) = 1.57 \;\; \mathsf{F}_{\mathsf{nl}}(15, 126) = 1.53 \qquad (5)$$

The forecasts are shown in Figure 14.7, with the top two panels recording the forecasts in differences and levels assuming a direct shift in 2010 modeled by a step shift in the intercept, and the bottom two panels record the forecasts for an induced shift in 2010 where the step indicator is interacted with lagged emissions. These results improve on those in Castle and Hendry (2022), with the main change being that the 2008 Climate Change Act also increased the speed of adjustment to the new equilibrium mean.

5. FORECASTING CLIMATE VARIABLES 20 YEARS AHEAD

Figure 14.1 plotted four of the key climate variables, namely atmospheric CO_2, global mean surface temperature deviations (*Temp*), ocean heat content deviations to 700 meters (*Ocean*), and global sea level rise (*Sea*), with data definitions and sources given in Table 14A.1. In this section, we select a simultaneous equations system (SEM) for them from a five-lag linear vector autoregression (VAR) over our longest common sample period, which is 1960–2018 after creating five lags, so $T = 59$. The VAR is first extended by testing for trend shifts, then restricted to significant variables in each equation, and finally expressed as an identified SEM with contemporaneous interactions. Its solved form enables long-term forecasts that are more sophisticated than the naïve forecasts in section 4.

The vector of variables is denoted by $\mathbf{y}_t = (CO_2, Temp, Ocean, Sea)_t$ and the VAR is[6]

$$\mathbf{y}_t = \boldsymbol{\pi}_0 + \sum_{j=1}^{5} \boldsymbol{\Pi}_j \mathbf{y}_{t-j} + \sum_{k=3}^{T-1} \boldsymbol{\lambda}_k \tau_{1959+k} + \boldsymbol{\nu}_t \qquad (6)$$

[6] Our forecasts are qualitatively similar if we use the log rather than level of CO_2, but we suggest instead using the log of CO_2 for a static or long-run conditional forecast, that is, one that forecasts temperature on the contemporaneous value of CO_2 concentrations (see Miller and Brock, 2024).

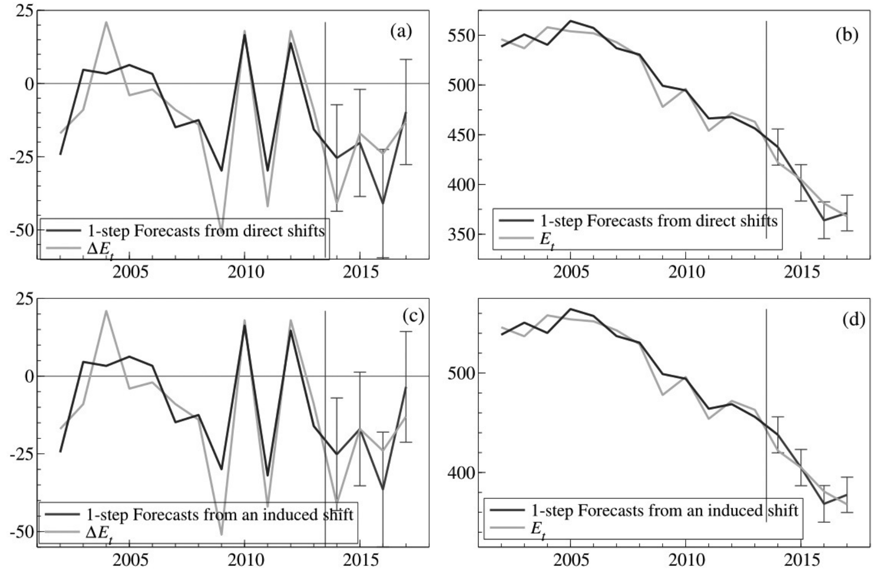

Figure 14.7 1-step ahead forecasts for change in emissions and level of emissions assuming all detected location shifts are direct shifts in the intercept (panels (a) and (b)); and where the retained step indicator in 2010 is interacted with the lagged dependent variable to model an induced shift in dynamics (panels (c) and (d))

Table 14.1 System diagnostic tests

$\mathsf{F}_{ar}(32, 152) = 0.89$	second-order vector residual autocorrelation
$\mathsf{F}_{arch}(16, 156) = 0.76$	first-order vector residual ARCH
$\chi^2_{nd}(8) = 10.7^*$	vector residual non-normality
$\mathsf{F}_{het}(72, 147) = 1.46^*$	vector residual heteroskedastcity
$\mathsf{F}_{reset}(32, 141) = 1.05$	RESET functional form
$\mathsf{F}_{nl}(108, 77) = 1.07$	nonlinearity index test

We use TIS to allow for the trend shifts apparent in Figure 14.1(b)–(d). The deterministic trends and shifts therein are proxies for economic activity aggregated across billions of individuals including all their fossil fuel use, agriculture and deforestation, construction and waste which while they are all stochastic, evolve slowly but with sudden shifts in growth due to crisies, pandemics, wars etc. (see Hendry, 1995, Chapter 15).

Table 14.2 Correlations between residuals (standard deviations on diagonal)

	CO_2	Temp	OceanHeat	SeaLevel
CO_2	0.37			
Temp	0.38	0.01		
OceanHeat	-0.02	-0.24	0.90	
SeaLevel	-0.16	-0.18	0.23	0.15

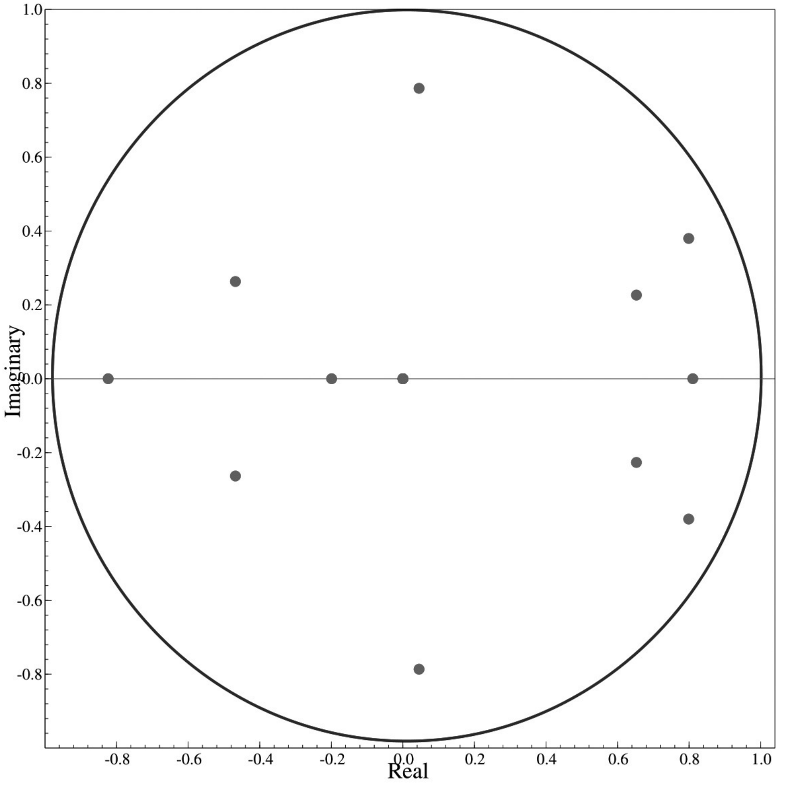

Figure 14.8 Eigenvalues of the dynamic system (7)–(10)

Selection for trend shifts was at $\alpha = 0.0001 = 0.01\%$ keeping all other regressors, retaining τ_{1991} and τ_{2003} which were significant on the system test. Next, lagged variables were selected by a system test at 1% in that specification, which reduced the maximum lag to four, leaving

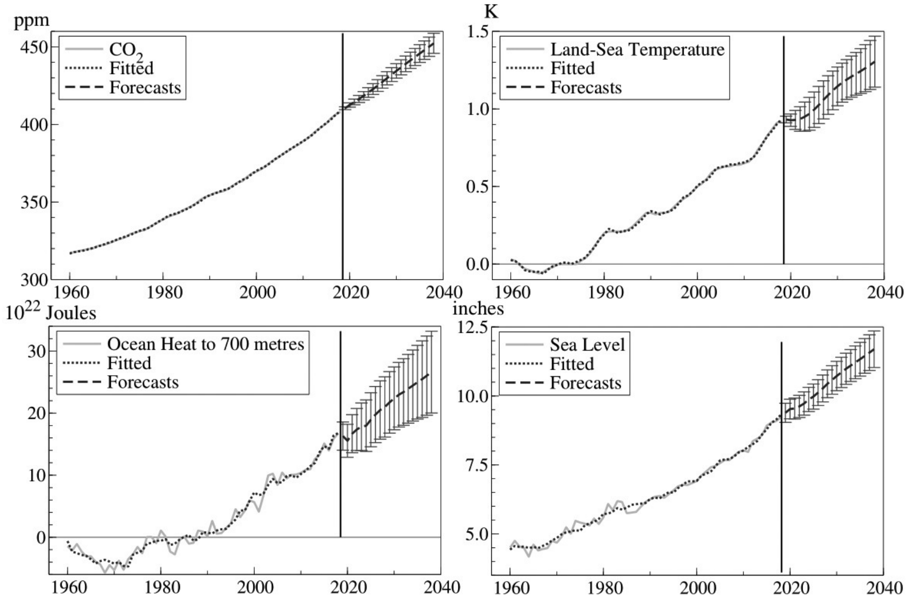

Figure 14.9 Actual and fitted values, and dynamic forecasts to 2038 all with $\pm 2\hat{\sigma}_f$: (a) Atmospheric CO_2 in parts per million (ppm); (b) annual global mean surface temperature deviations in degrees K; (c) ocean heat content deviations to 700 meters in 10^{22} Joules; (d) global sea level rise in inches

19 variables in each equation of (85). Next, regressors in each equation that were insignificant at 1% were eliminated separately (see Doornik and Hendry, 2022). In the resulting highly restricted system, all retained variables are significant at 1% both on individual and system tests so contemporaneous variables from other equations could be added without losing identification as the rank condition is imposed as a constraint (see Hendry and Krolzig, 2005). Only two proved significant and the resulting SEM is recorded in equations (7)–(10).

$$CO_{2,t} = \underset{(0.06)}{0.70}\ CO_{2,t-1} + \underset{(1.9)}{7.3}\ Temp_t - \underset{(0.27)}{0.68}\ Sea_{t-2} - \underset{(0.03)}{0.10}\ \tau_{1991} - \underset{(0.04)}{0.15}\ \tau_{2003} + \underset{(8.8)}{28.5} + \underset{(0.11)}{0.60}\ t \tag{7}$$

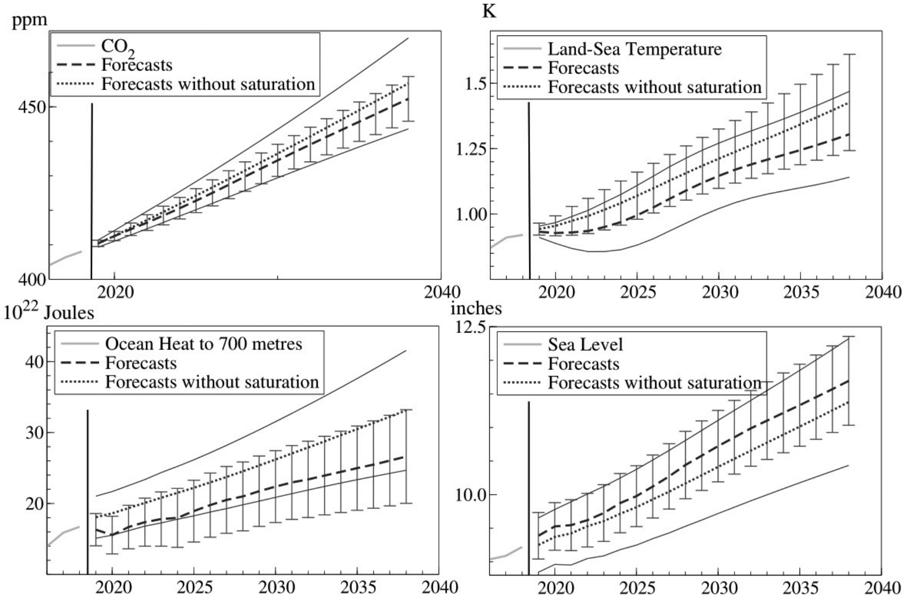

Figure 14.10 Dynamic forecasts to 2038 for the system with and without trend saturation all with $\pm 2\hat{\sigma}_f$ for (a) atmospheric CO_2 in parts per million (ppm); (b) annual global mean surface temperature deviations in degrees K; (c) ocean heat content deviations to 700 meters in 10^{22} Joules; (d) global sea level rise in inches

$$\begin{aligned} Temp_t = & \underset{(0.05)}{1.1}\ Temp_{t-1} - \underset{(0.06)}{0.57}\ Temp_{t-3} + \underset{(0.002)}{0.007}\ CO_{2,t-1} + \underset{(0.001)}{0.002}\ Ocean_{t-4} \\ & + \underset{(0.008)}{0.029}\ Sea_{t-3} + \underset{(0.0014)}{0.005}\ \tau_{2003} - \underset{(0.23)}{1.08} - \underset{(0.003)}{0.01}\ t \end{aligned} \tag{8}$$

$$\begin{aligned} Ocean_t = & \underset{(0.13)}{1.23}\ CO_{2,t} - \underset{(5)}{28.5}\ Temp_{t-3} + \underset{(0.10)}{0.30}\ Ocean_{t-4} + \underset{(0.79)}{3.52}\ Sea_{t-2} \\ & + \underset{(0.77)}{2.22}\ Sea_{t-3} + \underset{(0.13)}{0.94}\ \tau_{2003} - \underset{(16)}{127} - \underset{(0.28)}{2.47}\ t \end{aligned} \tag{9}$$

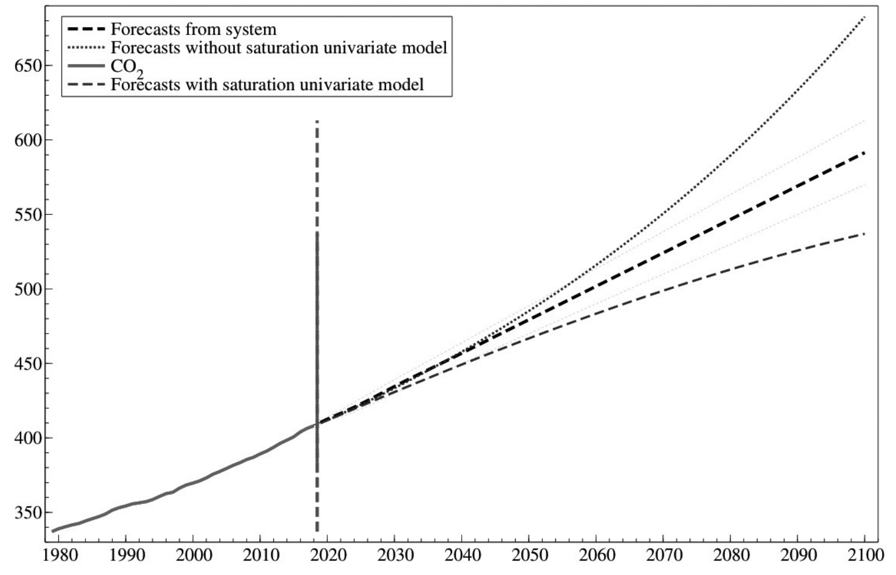

Figure 14.11 Forecasts of CO_2 to 2100 from system (thick dashed) compared to univariate forecasts without saturation (1) (dotted) and with saturation (2) (thin dashed)

$$Sea_t = \underset{(0.55)}{3.16}\ Temp_{t-1} - \underset{(0.014)}{0.063}\ CO_{2,t-1} - \underset{(0.015)}{0.028}\ Ocean_{t-4} + \underset{(0.12)}{0.15}\ Sea_{t-2} - \underset{(0.011)}{0.024}\ \tau_{1991} - \underset{(0.017)}{0.072}\ \tau_{2003} + \underset{(0.038)}{0.195}\ t \qquad (10)$$

The likelihood-ratio test of over-identifying restrictions against the restricted VAR (conducted on the restricted VAR to ensure the rank and order conditions for identification are satisfied, also see Hendry and Mizon, 1993) delivered $\chi^2(10) = 5.19$. None of the system diagnostic tests were significant at 1%, reported in Table 14.1, and no individual-equation index tests for nonlinearity (Castle and Hendry, 2010) show unmodeled nonlinearity.

Table 14.2 reports the correlations between the residuals with the equation standard deviations on the diagonal.

The key significant contemporaneous effects were positive effects of *Temp* on $CO_{2,t}$ in (7) and of $CO_{2,t}$ on $Ocean_t$ in (9). In addition, there was a positive feedback of lagged CO_2 on *Temp* in (8). The negative coefficients on τ_{1991} and τ_{2003} in (7) and (10) show that atmospheric CO_2 and sea levels were increasing slower earlier than can be explained by the other variables whereas temperatures and ocean heat were rising faster. The trends detected in the system for

CO_2 are not those detected in the single equation model, suggesting mis-specification in the univariate model which was observed through the diagnostic tests.

All the eigenvalues of the dynamics were less than unity as shown in Figure 14.8, so there are no unit roots in this representation, with all the non-stationarity coming from the approximating trends and trend shifts. Given the positive feedbacks, without controlling the levels of atmospheric CO_2, the system will spiral ever higher.

Finally, we computed 20-steps ahead dynamic forecasts from the system (7)–(10): apart from known deterministic terms, all the stochastic variables are endogenous noting that the trend shift variables are zero after their end dates. Figure 14.9 records their actual and fitted values, and dynamic forecasts to 2038. Absent future negative trend breaks, CO_2 levels are forecast to exceed 450ppm with temperatures rising by almost 0.5° and sea level rising by about 2.5 inches.

Trend saturation in-sample influences the long-run forecasts significantly, as seen in Figure 14.10 which records the forecasts from Figure 14.9 along with the resulting forecasts when the trend breaks are set to zero. Without saturation the deterministic trend is assumed constant throughout the sample and this results in a higher prediction of CO_2 levels of almost 460ppm with temperatures rising by a further 0.1° relative to the case with saturation. There is a significant upward effect on ocean heat content, but sea levels are predicted to be slightly lower. All forecast confidence intervals are larger without saturation. The trend breaks capture changing anthropogenic effects which, if omitted, result in a biased estimate of the deterministic trend driving the long-run forecasts.

How do these forecasts compare to our naïve forecasts? Figure 14.11 records the forecasts for CO_2 out to 2100 compared to the univariate statistical forecasts. Absent policy intervention, CO_2 levels are forecast to reach almost 600ppm by 2100 which is in between the two univariate statistical forecasts and roughly in line with RCP6.0.

6. CONCLUSION

Econometric methods have a useful role to play in climate modeling because outcomes are determined by human behavior interacting with the physical properties of the Earth's climate system. However, the time-series data generated by that interaction are non-stationary from both stochastic trends and location and trend shifts making forecasts uncertain and prone to failure howsoever they are generated. Unanticipated changes cannot be avoided but whether or not shifts that were once in the future were expected, they later become in-sample, so empirical modeling must take account of them to avoid distortions in parameter estimates and the resulting forecasts. This chapter sought to explain climate changes, and forecasting in non-stationary processes, emphasizing how location shifts could be identified and how doing so improved the verisimilitude of the model and its forecasts, although nothing precludes new unanticipated shifts.

However, climate change is not a given but is an anthropogenic outcome, so it is possible to get to net-zero GHG emissions by 2050 (see e.g., Castle and Hendry, 2024a, 2024b). The speed and form of such a transition will impact on climate forecasting, including risks of a disorderly adjustment in financial markets. Following its Climate Change Act of 2008 (CCA08) the UK had made good progress in GHG emissions reductions, but Miller and Brock (2024) show that the risk of mortality in London is barely affected if the UK acts alone and without adaptation. Future COPs will need far greater success than achieved to date to avoid serious problems given the extreme weather events already witnessed. The consensus coming out of the recent COP28 in the United Arab Emirates is a small step in the right direction.

ACKNOWLEDGEMENTS

Financial support from the Robertson Foundation (award 9907422) and Nuffield College is gratefully acknowledged, as are important contributions to the background research from William A. Brock, Susana Campos-Martins, Jurgen A. Doornik, Luke P. Jackson, Søren Johansen, Andrew B. Martinez, Bent Nielsen and Felix Pretis. All calculations and graphs use PcGive and OxMetrics. Prepared for the *Handbook of Research Methods and Applications in Macroeconomic Forecasting*, Michael P. Clements and Ana Galvão (Eds), with thanks for their helpful comments.

REFERENCES

Arrhenius, S. A. (1896). On the influence of carbonic acid in the air upon the temperature of the ground. *London, Edinburgh, and Dublin Philosophical Magazine and Journal of Science (fifth series) 41*, 237–275. https://doi.org/10.1080/14786449608620846.

Azar, C. and T. Sterner (1996). Discounting and distributional considerations in the context of global warming. *Ecological Economics 19*, 169–184. https://doi.org/10.1016/0921-8009(96)00065-1.

Baek, Y. (2019). Forecasting in long horizons using smoothed direct forecast. *Journal of Forecasting 38*, 277–292. https://doi.org/10.1002/for.2572

Bai, J. and P. Perron (1998). Estimating and testing linear models with multiple structural changes. *Econometrica 66*, 47–78. https://doi.org/10.2307/2998540.

Bloemendaal, N., H. de Moel, and A. B. Martinez (2022). A globally consistent local-scale assessment of future tropical cyclone risk. *Science Advances 8*. https://www.science.org/doi/abs/10.1126/sciadv.abm8438.

Boyer, G. R. and T. J. Hatton (2002). New estimates of British unemployment, 1870–1913. *Journal of Economic History 62*, 643–675. https://doi.org/10.1017/S0022050702001031.

Brock, W. A. and J. I. Miller (2023). Polar amplification in a moist energy balance model: A structural econometric approach to estimation and testing. SSRN working paper. http://dx.doi.org/10.2139/ssrn.4450492.

Brock, W. A. and A. Xepapadeas (2017). Climate change policy under polar amplification. *European Economic Review 94*, 263–282. https://doi.org/10.1016/j.euroecorev.2017.06.008.

Bruns, S. B., Z. Csereklyei, and D. I. Stern (2020). A multicointegration model of global climate change. *Journal of Econometrics 214*, 175–197. https://doi.org/10.1016/j.jeconom.2019.05.010.

Budyko, M. I. (1969). The effect of solar radiation variations on the climate of the Earth. *Tellus 21*, 611–619. https://doi.org/10.1111/j.2153-3490.1969.tb00466.x.

Castle, J. L., M. P. Clements, and D. F. Hendry (2015a). Robust approaches to forecasting. *International Journal of Forecasting 31*, 99–112. https://doi.org/10.1016/j.ijforecast.2014.11.002.

Castle, J. L., J. A. Doornik, and D. F. Hendry (2021a). Forecasting principles from experience with forecasting competitions. *Forecasting 3(1)*, 138–165. https://www.mdpi.com/2571-9394/3/1/10.

Castle, J. L., J. A. Doornik, and D. F. Hendry (2021b). Selecting a model for forecasting. *Econometrics 9(3)*, https://doi.org/10.3390/econometrics9030026.

Castle, J. L., J. A. Doornik, and D. F. Hendry (2023). Improving models and forecasts after equilibrium-mean shifts. *International Journal of Forecasting 40(3)*, 1085–1100. https://doi.org/10.1016/j.ijforecast.2023.09.006.

Castle, J. L., J. A. Doornik, D. F. Hendry, and F. Pretis (2015b). Detecting location shifts during model selection by step-indicator saturation. *Econometrics 3(2)*, 240–264. https://doi.org/10.3390/econometrics3020240.

Castle, J. L., J. A. Doornik, D. F. Hendry, and F. Pretis (2019). Trend-indicator saturation. Working paper, Nuffield College, Oxford University.

Castle, J. L., N. W. P. Fawcett, and D. F. Hendry (2010). Forecasting with equilibrium-correction models during structural breaks. *Journal of Econometrics 158*, 25–36. https://doi.org/10.1016/j.jeconom.2010.03.004.

Castle, J. L., N. W. P. Fawcett, and D. F. Hendry (2011). Forecasting breaks and during breaks. In M. P. Clements and D. F. Hendry (Eds.), *Oxford Handbook of Economic Forecasting*, pp. 315–353. Oxford: Oxford University Press.

Castle, J. L. and D. F. Hendry (2010). A low-dimension portmanteau test for non-linearity. *Journal of Econometrics 158(2)* 231–245, https://doi.org/10.1016/j.jeconom.2010.01.006.

Castle, J. L. and D. F. Hendry (2022). Econometrics for modelling climate change. In J. Hamilton (Ed.), *Oxford Research Encyclopedia of Economics and Finance*. Oxford: Oxford University Press. https://doi.org/10.1093/acrefore/9780190625979.013.675.

Castle, J. L. and D. F. Hendry (2024a). Can the UK achieve net-zero Greenhouse Gas emissions by 2050? National Institute Economic Review, 1-11. https://doi.org/10.1017/nie.2024.6.

Castle, J. L. and D. F. Hendry (2024b). Five sensitive intervention points to achieve climate neutrality by 2050, illustrated by the UK. Renewable Energy, 226, 120445. https://doi.org/10.1016/j.renene.2024.120445.

Castle, J. L., D. F. Hendry, and A. B. Martinez (2017). Evaluating forecasts, narratives and policy using a test of invariance. *Econometrics 5(39)*, https://doi.org/10.3390/econometrics5030039.

Castruccio, S., D. J. McInerney, M. L. Stein, F. L. Crouch, R. L. Jacob, and E. J. Moyer (2014). Statistical emulation of climate model projections based on precomputed GCM runs. *Journal of Climate 27*, 1829–1844. https://doi.org/10.1175/JCLI-D-13-00099.1.

Chang, Y., R. K. Kaufmann, C. S. Kim, J. I. Miller, J. Y. Park, and S. Park (2020). Evaluating trends in time series of distributions: A spatial fingerprint of human effects on climate. *Journal of Econometrics 214*, 274–294. https://doi.org/10.1016/j.jeconom.2019.05.014.

Cheng, C.-H. and S. A. T. Redfern (2022). Impact of interannual and multidecadal trends on methane-climate feedbacks and sensitivity. *Nature Communications*. https://doi.org/10.1038/s41467-022-31345-w.

Chow, G. C. (1960). Tests of equality between sets of coefficients in two linear regressions. *Econometrica 28*, 591–605. https://doi.org/10.2307/1910133.

Church, J. A. and N. J. White (2011). Sea-level rise from the late 19th to the early 21st century. *Surveys in Geophysics 32*, 585–602. http://doi.org/10.1007/s10712-011-9119-1.

Claussen, M., L. Mysak, A. Weaver, M. Crucifix, T. Fichefet, M.-F. Loutre, S. Weber, J. Alcamo, V. Alexeev, A. Berger, R. Calov, A. Ganopolski, H. Goosse, G. Lohmann, F. Lunkeit, I. Mokhov, V. Petoukhov, P. Stone, and Z. Wang (2002). Earth system models of intermediate complexity: Closing the gap in the spectrum of climate system models. *Climate Dynamics 18*, 579–586. https://doi.org/10.1007/s00382-001-0200-1.

Clements, M. P. and D. F. Hendry (1998). *Forecasting Economic Time Series*. Cambridge: Cambridge University Press.

Davidson, J. E. H., D. B. Stephenson, and A. A. Turasie (2016). Time series modeling of paleoclimate data. *Environmetrics 27*, 55–65. https://doi.org/10.1002/env.2373.

Diebold, F. X. and G. D. Rudebusch (2022). Probability assessments of an ice-free Arctic: Comparing statistical and climate model projections. *Journal of Econometrics 231*, 520–534. https://www.sciencedirect.com/science/article/pii/S0304407620304012

Dietz, S., F. van der Ploeg, A. Rezai, and F. Venmans (2021). Are economists getting climate dynamics right and does it matter? *Journal of the Association of Environmental and Resource Economists 8*, 895–921. https://doi.org/10.1086/713977.

Doornik, J. A. (2009). Autometrics. In J. L. Castle and N. Shephard (Eds.), *The Methodology and Practice of Econometrics*, pp. 88–121. Oxford: Oxford University Press.

Doornik, J. A. and H. Hansen (2008). An omnibus test for univariate and multivariate normality. *Oxford Bulletin of Economics and Statistics 70*, 927–939. https://doi.org/10.1111/j.1468-0084.2008.00537.x.

Doornik, J. A. and D. F. Hendry (2022). *Modelling Dynamic Systems using PcGive: Volume II* (9th ed.). London: Timberlake Consultants Press.

Engle, R. F. (1982). Autoregressive conditional heteroscedasticity, with estimates of the variance of United Kingdom inflation. *Econometrica 50*, 987–1007. https://doi.org/10.2307/1912773.

Engle, R. F. and D. F. Hendry (1993). Testing super exogeneity and invariance in regression models. *Journal of Econometrics 56*, 119–139. https://doi.org/10.1016/0304-4076(93)90103-C.

Engle, R. F., D. F. Hendry and J.-F. Richard (1983). Exogeneity. *Econometrica 51*, 277–304. https://doi.org/10.2307/1911990.

Environment Agency (2011). Coastal flood boundary conditions for UK mainland and islands. https://assets.publishing.service.gov.uk/media/603653898fa8f5481378420b/Design_sea_levels_technical_report.pdf

Ericsson, N. R. (2012). Detecting crises, jumps, and changes in regime. Working paper, Federal Reserve Board of Governors, Washington, D.C. https://eesp.fgv.br/sites/eesp.fgv.br/files/file/Neil_Ericsson.pdf

Ericsson, N. R., M. H. I. Dore, and H. Butt (2022). Detecting and quantifying structural breaks in climate. *Econometrics 10*, 33. https://doi.org/10.3390/econometrics10040033.

Estrada, F. and P. Perron (2014). Detection and attribution of climate change through econometric methods. *Boletín de la Sociedad Matemática Mexicana 20*, 107–136. https://doi.org/10.1007/s40590-014-0009-7.

Estrada, F., P. Perron, C. Gay-García, and B. Martínez-López (2013a). A time-series analysis of the 20th century climate simulations produced for the IPCC's Fourth Assessment Report. *PLoS ONE 8*, e60017. https://doi.org/10.1371/journal.pone.0060017.

Estrada, F., P. Perron, and B. Martínez-López (2013b). Statistically derived contributions of diverse human influences to twentieth-century temperature changes. *Nature Geoscience 6*, 1050–1055. https://doi.org/10.1038/ngeo1999.

Fawcett, A. A., G. C. Iyer, L. E. Clarke, J. A. Edmonds, N. E. Hultman, H. C. McJeon, J. Rogelj, R. Schuler, J. Alsalam, G. R. Asrar, J. Creason, M. Jeong, J. McFarland, A. Mundra, and W. Shi (2015). Can Paris pledges avert severe climate change? Reducing risks of severe outcomes and improving chances of limiting warming to 2°C. *Science 350*, 1168–1169. https://doi.org/10.1126/science.aad5761.

Foote, E. (1856). Circumstances affecting the heat of the sun's rays. *The American Journal of Science and Arts 22*, 382–383. https://www.proquest.com/scholarly-journals/art-xxxi-circumstances-affecting-heat-suns-rays/docview/89589867/se-2.

Francis, J. A. and S. J. Vavrus (2012). Evidence linking Arctic amplification to extreme weather in mid-latitudes. *Geophysical Research Letters 39*, L06801. https://doi.org/10.1029/2012GL051000.

Giacomini, R. and B. Rossi (2009). Detecting and predicting forecast breakdowns. *Review of Economic Studies 76*, 669–705. https://doi.org/10.1111/j.1467-937X.2009.00545.x.

Godfrey, L. G. (1978). Testing for higher order serial correlation in regression equations when the regressors include lagged dependent variables. *Econometrica 46*, 1303–1313. https://doi.org/10.2307/1913830.

Granger, C. W. J. and T. Lee (1990). Multicointegration. In G. F. Rhodes and T. B. Fomby (Eds.), *Advances in Econometrics*, Volume 8. Greenwich, CT: JAI Press.

Hansen, J., M. Sato, P. Kharecha, K. von Schuckmann, D. J. Beerling, J. Cao, S. Marcott, V. Masson-Delmotte, M. J. Prather, E. J. Rohling, J. Shakun, P. Smith, A. Lacis, G. Russell, and R. Ruedy (2017). Young people's burden: Requirement of negative CO_2 emissions. *Earth System Dynamics 8*, 577–616. https://doi.org/10.5194/esd-8-577-2017.

Hausfather, Z. and G. P. Peters (2020). Emissions – the 'business as usual' story is misleading. *Nature 577*, 618–620. https://doi.org/10.1038/d41586-020-00177-3.

Held, I. M. and M. J. Suarez (1974). Simple albedo feedback models of the icecaps. *Tellus 26*, 613–629. https://doi.org/10.1111/j.2153-3490.1974.tb01641.x.

Held, I. M., M. Winton, K. Takahashi, T. Delworth, F. Zeng, and G. K. Vallis (2010). Probing the fast and slow components of global warming by returning abruptly to preindustrial forcing. *Journal of Climate 23*, 2418–2427. https://doi.org/10.1175/2009JCLI3466.1.

Hendry, D. F. (1995). *Dynamic Econometrics*. Oxford: Oxford University Press.

Hendry, D. F. (1997). The econometrics of macroeconomic forecasting. *Economic Journal 107*, 1330–1357. https://doi.org/10.1111/j.1468-0297.1997.tb00051.x.

Hendry, D. F. (2006). Robustifying forecasts from equilibrium-correction models. *Journal of Econometrics 135*, 399–426. https://doi.org/10.1016/j.jeconom.2005.07.029.

Hendry, D. F. and M. P. Clements (2004). Pooling of forecasts. *Econometrics Journal 7*, 1–31. https://doi.org/10.1111/j.1368-423X.2004.00119.x.

Hendry, D. F., S. Johansen, and C. Santos (2008). Automatic selection of indicators in a fully saturated regression. *Computational Statistics 23(2)*, 317–335, Erratum, 337–339. https://doi.org/10.1007/s00180-007-0054-z

Hendry, D. F. and H.-M. Krolzig (2005). The properties of automatic Gets modelling. *Economic Journal 115*, C32–C61. https://doi.org/10.1111/j.0013-0133.2005.00979.x

Hendry, D. F. and G. E. Mizon (1993). Evaluating dynamic econometric models by encompassing the VAR. In P. C. B. Phillips (Eds.), *Models, Methods and Applications of Econometrics* pp. 272–300. Oxford: Basil Blackwell.

Hendry, D. F. and G. E. Mizon (2012). Open-model forecast-error taxonomies. In X. Chen and N. R. Swanson (Eds.), *Recent Advances and Future Directions in Causality, Prediction, and Specification Analysis*, pp. 219–240. New York: Springer.

Hendry, D. F. and F. Pretis (2023). Analyzing differences between scenarios. *International Journal of Forecasting 39*, 754–771. https://doi.org/10.1016/j.ijforecast.2022.02.004.

Huntingford, C., H. Yang, A. Harper, P. M. Cox, N. Gedney, E. J. Burke, J. A. Lowe, G. Hayman, W. J. Collins, S. M. Smith, and E. Comyn-Platt (2017). Flexible parameter-sparse global temperature time profiles that stabilise at 1.5 and 2.0 °C. *Earth System Dynamics 8*, 617–626. https://doi.org/10.5194/esd-8-617-2017.

Inoue, A., L. Jin, and B. Rossi (2017). Rolling window selection for out-of-sample forecasting with time-varying parameters. *Journal of Econometrics 196*, 55–67. https://doi.org/10.1016/j.jeconom.2016.03.006.

IPCC (2014a). Anthropogenic and natural radiative forcing. In *Climate Change 2013 – The Physical Science Basis: Working Group I Contribution to the Fifth Assessment Report of the Intergovernmental Panel on Climate Change*, pp. 659–740. Cambridge, UK: Cambridge University Press. https://doi.org/10.1017/CBO9781107415324.018.

IPCC (2014b). Clouds and aerosols. In *Climate Change 2013 – The Physical Science Basis: Working Group I Contribution to the Fifth Assessment Report of the Intergovernmental Panel on Climate Change*, pp. 571–658. Cambridge, UK: Cambridge University Press. https://doi.org/10.1017/CBO9781107415324.016.

Ivanov, M. A., J. Luterbacher, and S. Kotlarski (2018). Climate model biases and modification of the climate change signal by intensity-dependent bias correction. *Journal of Climate 31*, 6591–6610. https://doi.org/10.1175/JCLI-D-17-0765.1.

Jackson, L., K. Juselius, A. B. Martinez, and F. Pretis (2021). Modeling the interconnectivity of non-stationary polar ice sheets. Discussion paper, SSRN, https://ssrn.com/abstract=3912725.

Jackson, L. P., A. Grinsted, and S. Jevrejeva (2018). 21st century sea-level rise in line with the Paris Accord. *Earth's Future*, https://doi.org/10.1002/2017EF000688.

Jackson, L. P. and D. F. Hendry (2018). Risk and exposure of coastal cities to future sea-level rise. Working paper, INET Oxford, Oxford University.

Jackson, L. P. and S. Jevrejeva (2016). A probabilistic approach to 21st century regional sea-level projections using RCP and upper-limit scenarios. *Global and Planetary Change 146*, 179–189. https://doi.org/10.1016/j.gloplacha.2016.10.006.

Jevrejeva, S., L. P. Jackson, A. Grinsted, D. Lincke, and B. Marzeion (2018). Flood damage costs under the sea level rise with warming of 1.5 °C and 2 °C. *Environmental Research Letters 13*, https://doi.org/10.1088/1748–9326/aacc76.

Jevrejeva, S., H. Palanisamy, and L. P. Jackson (2020). Global mean thermosteric sea level projections by 2100 in CMIP6 climate models. *Environmental Research Letters 16*. https://doi.org/10.1088/1748-9326/abceea.

Kaufmann, R. K. (1997). Assessing the DICE model: Uncertainty associated with the emission and retention of greenhouse gases. *Climatic Change 35*, 435–448. https://doi.org/10.1023/A:1005372513452.

Kaufmann, R. K., H. Kauppi, M. L. Mann, and J. H. Stock (2011). Reconciling anthropogenic climate change with observed temperature 1998–2008. *Proceedings of the National Academy of Sciences 108*, 11790–11793. https://doi.org/10.1073/pnas.1102467108.

Kaufmann, R. K., H. Kauppi, M. L. Mann, and J. H. Stock (2013). Does temperature contain a stochastic trend: Linking statistical results to physical mechanisms. *Climatic Change 118*, 729–743. https://doi.org/10.1007/s10584-012-0683-2.

Kaufmann, R. K., H. Kauppi, and J. H. Stock (2006a). Emissions, concentrations and temperature: A time series analysis. *Climatic Change 77*, 249–278. https://doi.org/10.1007/s10584-006-9062-1.

Kaufmann, R. K., H. Kauppi, and J. H. Stock (2006b). The relationship between radiative forcing and temperature: What do statistical analyses of the instrumental temperature record measure? *Climatic Change 77*, 279–289. https://doi.org/10.1007/s10584-006-9063-0.

Kaufmann, R. K., H. Kauppi, and J. H. Stock (2010). Does temperature contain a stochastic trend? Evaluating conflicting statistical results. *Climatic Change 101*, 395–405. https://doi.org/10.1007/s10584-009-9711-2.

Kaufmann, R. K. and D. I. Stern (2002). Cointegration analysis of hemispheric temperature relations. *Journal of Geophysical Research 107*, 4012. https://doi.org/10.1029/2000JD000174.

Keeling, C. D., R. B. Bacastow, A. E. Brainbridge, C. A. Ekdahl, P. R. Guenther, L. S. Waterman, and J. F. S. Chin (1976). Atmospheric carbon dioxide variations at Mauna Loa observatory, Hawaii. *Tellus 6*, 538–551. https://doi.org/10.3402/tellusa.v28i6.11322.

Kitov, O. I. and M. N. Tabor (2015). Detecting structural changes in linear models: A variable selection approach using multiplicative indicator saturation. Unpublished paper, University of Oxford.

Knutti, R., R. Furrer, C. Tebaldi, J. Cermak, and G. A. Meehl (2010). Challenges in combining projections from multiple climate models. *Journal of Climate 23*, 2739–2758. https://doi.org/10.1175/2009JCLI3361.1.

Kosaka, Y. and S.-P. Xie (2013). Recent global-warming hiatus tied to equatorial Pacific surface cooling. *Nature 501*, 403–407. https://doi.org/10.1038/nature12534.

Kulp, S. A. and B. H. Strauss (2019). New elevation data triple estimates of global vulnerability to sea-level rise and coastal flooding. *Nature Communications 10*. https://doi.org/10.1038/s41467-019-12808-z.

Langen, P. L. and V. I. Alexeev (2007). Polar amplification as a preferred response in an idealized aquaplanet GCM. *Climate Dynamics 29*, 305–317. https://doi.org/10.1007/s00382-006-0221-x.

Lavers, D. A., M. J. Rodwell, D. S. Richardson, and et al. (2018). The gauging and modeling of rivers in the sky. *Geophysical Research Letters 45*, 7828–7834. https://doi.org/10.1029/2018GL079019.

Leduc, M., H. D. Matthews, and R. de Elía (2016). Regional estimates of the transient climate response to cumulative CO_2 emissions. *Nature Climate Change 6*, 474–478. https://doi.org/10.1038/nclimate2913.

Levitus, S., J. Antonov, T. Boyer, R. Locarnini, H. Garcia, and A. Mishonov (2009). Global ocean heat content 1955–2008 in light of recently revealed instrumentation problems. *Geophysical Research Letters 36(7)*, https://doi.org/10.1029/2012GL051106.

Lopez, A., E. B. Suckling, and L. A. Smith (2014). Robustness of pattern scaled climate change scenarios for adaptation decision support. *Climatic Change 122*, 555–566. https://doi.org/10.1007/s10584-013-1022-y.

Lunsford, K. G. and D. West, K (2021). An empirical evaluation of some long-horizon macroeconomic forecasts. *National Bureau of Economic Research 18*. https://www.nber.org/sites/default/files/2022-02/NB21-18

Martinez, A. B. (2020). Forecast accuracy matters for hurricane damages. *Econometrics 8(2)*, https://doi.org/10.3390/econometrics8020018.

Martinez, A. B., J. L. Castle, and D. F. Hendry (2022). Smooth robust multi-horizon forecasts. *Advances in Econometrics 43A*, 143–165. https://doi.org/10.1108/S0731-90532021000043A008.

Matthews, H. D., N. P. Gillett, P. Stott, and K. Zickfeld (2009). The proportionality of global warming to cumulative carbon emissions. *Nature 459*, 829–832. https://doi.org/10.1038/nature08047.

Meinshausen, M., S. C. B. Raper, and T. M. L. Wigley (2011). Emulating coupled atmosphere-ocean and carbon cycle models with a simpler model, MAGICC6. Part 1: Model description and calibration. *Atmospheric Chemistry and Physics 11*, 1417–1456. https://doi.org/10.5194/acp-11-1417-2011.

Merlis, T. M. and M. Henry (2018). Simple estimates of polar amplification in moist diffusive energy balance models. *Journal of Climate 31*, 5811–5824. https://doi.org/10.1175/JCLI-D-17-0578.1.

Miftakhova, A., K. L. Judd, T. S. Lontzek, and K. Schmedders (2020). Statistical approximation of high-dimensional climate models. *Journal of Econometrics 214*, 67–80. https://doi.org/10.1016/j.jeconom.2019.05.005.

Miller, J. I. and W. A. Brock (2024). Beyond RCP8.5: Marginal mitigation using quasi-representative concentration pathways. *Journal of Econometrics*, *239(1)*, article 105152. https://doi.org/10.1016/j.jeconom.2021.06.007.

Miller, J. I. and K. Nam (2020). Dating hiatuses: A statistical model of the recent slowdown in global warming and the next one. *Earth System Dynamics 11*, 1123–1132.

https://doi.org/10.5194/esd-11-1123-2020.
Monier, E., S. Paltsev, A. Sokolov, Y.-H. H. Chen, X. Gao, Q. Ejaz, E. Couzo, C. Schlosser, S. Dutkiewicz, C. Fant, J. Scott, D. Kicklighter, J. Morris, H. Jacoby, and M. Prinn, R. Haigh (2018). Toward a consistent modeling framework to assess multi-sectoral climate impacts. *Nature Communications 9*, 660. https://doi.org/10.1038/s41467-018-02984-9.
Moss, R. H., J. A. Edmonds, K. A. Hibbard, M. R. Manning, S. K. Rose, D. P. van Vuuren, T. R. Carter, S. Emori, M. Kainuma, T. Kram, G. A. Meehl, J. F. B. Mitchell, N. Nakicenovic, K. Riahi, S. J. Smith, R. J. Stouffer, A. M. Thomson, J. P. Weyant, and T. J. Wilbanks (2010). The next generation of scenarios for climate change research and assessment. *Nature 463*, 747–756. https://doi.org/10.1038/nature08823.
Müller, U. K. and M. W. Watson (2016). Measuring uncertainty about long-run predictions. *Review of Economic Studies 83*, 1711–1740. https://doi.org/10.1093/restud/rdw003
Nordhaus, W. (1993). Rolling the 'DICE': An optimal transition path for controlling greenhouse gases. *Resource and Energy Economics 15*, 27–50. https://doi.org/10.1016/0928-7655(93)90017-O.
Nordhaus, W. D. (2013). *The Climate Casino: Risk, Uncertainty, and Economics for a Warming World*. New Haven: Yale University Press. https://www.jstor.org/stable/j.ctt5vkrpp.
North, G. R. (1975). Theory of energy-balance climate models. *Journal of Atmospheric Sciences 32*, 2033–2043. https://doi.org/10.1175/1520-0469(1975)032<2033:TOEBCM>2.0.CO;2.
North, G. R. and R. F. Cahalan (1981). Predictability in a solvable stochastic climate model. *Journal of the Atmospheric Sciences 38*, 504–513. https://doi.org/10.1175/1520-0469(1981)038<0504:PIASSC>2.0.CO;2.
North, G. R., R. F. Cahalan, and J. A. Coakley, Jr. (1981). Energy balance climate models. *Reviews of Geophysics and Space Physics 19*, 91–121. https://doi.org/10.1029/RG019i001p00091.
North, G. R., J. G. Mengel, and D. A. Short (1983). Simple energy balance model resolving the seasons and the continents: Application to the astronomical theory of the ice ages. *Journal of Geophysical Research 88*, 6576–6586. https://doi.org/10.1029/JC088iC11p06576.
Palmer, T. (2006). The primacy of doubt. *Physics World 19*, 38–39. https://iopscience.iop.org/article/10.1088/2058-7058/19/11/35.
Palmer, T. (2022). *The Primacy of Doubt: From Quantum Physics to Climate Change, How the Science of Uncertainty Can Help Us Understand Our Chaotic World*. Oxford: University of Oxford.
Pesaran, M. H., A. Pick, and M. Pranovich (2013). Optimal forecasts in the presence of structural breaks. *Journal of Econometrics 177*, 134–152. https://doi.org/10.1016/j.jeconom.2013.04.002.
Pesaran, M. H. and A. Timmermann (2007). Selection of estimation window in the presence of breaks. *Journal of Econometrics 137*, 134–161. https://doi.org/10.1016/j.jeconom.2006.03.010.
Poppick, A., E. J. Moyer, and M. L. Stein (2017). Estimating trends in the global mean temperature record. *Advances in Statistical Climatology, Meteorology, and Oceanography 3*, 33–53. https://doi.org/10.5194/ascmo-3-33-2017.

Pretis, F. (2020). Econometric modelling of climate systems: The equivalence of energy balance models and cointegrated vector autoregressions. *Journal of Econometrics 214*, 256–273. https://doi.org/10.1016/j.jeconom.2019.05.013.

Pretis, F. (2021). Exogeneity in climate econometrics. *Energy Economics 96*. https://doi.org/10.1016/j.eneco.2021.105122.

Pretis, F. and D. F. Hendry (2013). Comment on 'Polynomial cointegration tests of anthropogenic impact on global warming' by Beenstock et al. (2012) – Some hazards in econometric modelling of climate change. *Earth System Dynamics 4*, 375–384. https://esd.copernicus.org/articles/4/375/2013/.

Ramsey, J. B. (1969). Tests for specification errors in classical linear least squares regression analysis. *Journal of the Royal Statistical Society B 31*, 350–371. https://www.jstor.org/stable/2984219.

Rasmussen, D., M. Meinshausen, and R. Kopp (2016). Probability-weighted ensembles of U.S. county-level climate projections for climate risk analysis. *Journal of Applied Meteorology and Climatology 55*, 2301–2322. https://doi.org/10.1175/jamc-d-15-0302.1.

Riahi, K., S. Rao, V. Krey, C. Cho, V. Chirkov, G. Fischer, G. Kindermann, N. Nakicenovic, and P. Rafaj (2011). RCP 8.5 – A scenario of comparatively high greenhouse gas emissions. *Climatic Change 109*, 33. https://doi.org/10.1007/s10584-011-0149-y.

Riahi, K., D. P. van Vuuren, E. Kriegler, J. Edmonds, B. C. O'Neill, S. Fujimori, N. Bauer, K. Calvin, R. Dellink, O. Fricko, W. Lutz, A. Popp, J. C. Cuaresma, K. C. Samir, M. Leimbach, L. Jiang, T. Kram, S. Rao, J. Emmerling, K. Ebi, T. Hasegawa, P. Havlik, F. Humpenöder, L. A. Da Silva, S. Smith, E. Stehfest, V. Bosetti, J. Eom, D. Gernaat, T. Masui, J. Rogelj, J. Strefler, L. Drouet, V. Krey, G. Luderer, M. Harmsen, K. Takahashi, L. Baumstark, J. C. Doelman, M. Kainuma, Z. Klimont, G. Marangoni, H. Lotze-Campen, M. Obersteiner, A. Tabeau, and M. Tavoni (2017). The shared socioeconomic pathways and their energy, land use, and greenhouse gas emissions implications: An overview. *Global Environmental Change 42*, 153–168. https://doi.org/10.1016/j.gloenvcha.2016.05.009.

Ricke, K. L. and K. Caldeira (2014). Maximum warming occurs about one decade after a carbon dioxide emission. *Environmental Research Letters 9*, 124002. https://dx.doi.org/10.1088/1748-9326/9/12/124002.

Santer, B. D., T. M. L. Wigley, M. E. Schlesinger, and J. F. B. Mitchell (1990). Developing climate scenarios from equilibrium GCM results. Report 047, Max-Planck-Institut für Meteorologie. https://hdl.handle.net/21.11116/0000-0001-68B8-B.

Schmith, T., S. Johansen, and P. Thejll (2012). Statistical analysis of global surface temperature and sea level using cointegration methods. *Journal of Climate 25*, 7822–7833. https://doi.org/10.1175/JCLI-D-11-00598.1.

Schwartz, S. E. (2012). Determination of Earth's transient and equilibrium climate sensitivities from observations over the twentieth century: Strong dependence on assumed forcing. *Surveys in Geophysics 33*, 745–777. https://doi.org/10.1007/s10712-012-9180-4.

Sellers, W. D. (1969). A global climatic model based on the energy balance of the Earth-atmosphere system. *Journal of Applied Meteorology 8*, 392–400. https://doi.org/10.1175/1520-0450(1969)008<0392:AGCMBO>2.0.CO;2.

Sellers, W. D. (1976). A two-dimensional global climatic model. *Monthly Weather Review 104*, 233–248. https://doi.org/10.1175/1520-0493(1976)104<0233:ATGCM>2.0.CO;2.

Siler, N., G. H. Roe, and K. C. Armour (2018). Insights into the zonal-mean response of the hydrologic cycle to global warming from a diffusive energy balance model. *Journal of Climate 31*, 7481–7493. https://doi.org/10.1175/JCLI-D-18-0081.1.

Smith, M. R. and S. S. Myers (2018). Impact of anthropogenic CO2 emissions on global human nutrition. *Nature Climate Change*, doi:10.1038/s41558–018–0253–3.

Sokolov, A., D. Kicklighter, A. Schlosser, C. Wang, E. Monier, B. Brown-Steiner, R. Prinn, C. Forest, X. Gao, A. Libardoni, and S. Eastham (2018). Description and evaluation of the MIT Earth System Model (MESM). *Journal of Advances in Modeling Earth Systems 10*, 1759–1789. https://doi.org/10.1029/2018MS001277.

Stern, D. I. and R. K. Kaufmann (2000). Detecting a global warming signal in hemispheric temperature series: A structural time series analysis. *Climatic Change 47*, 411–438. https://doi.org/10.1023/A:1005672231474.

Stern, D. I. and R. K. Kaufmann (2014). Anthropogenic and natural causes of climate change. *Climatic Change 122*, 257–269. https://doi.org/10.1007/s10584-013-1007-x.

Sundquist, E. T. and R. F. Keeling (2009). The Mauna Loa carbon dioxide record: Lessons for long-term earth observations. In B. J. Mcpherson and E. T. Sundquist (Eds.), *Carbon Sequestration and Its Role in the Global Carbon Cycle*, Volume 183, pp. 27–35. Geophysical Monograph Series: American Geophysical Union. https://agupubs.onlinelibrary.wiley.com/doi/book/10.1029/GM183.

Tebaldi, C. and R. Knutti (2007). The use of the multi-model ensemble in probabilistic climate projections. *Philosophical Transactions of the Royal Society A 365*, 2053–2075. https://doi.org/10.1098/rsta.2007.2076.

Tebaldi, C. and R. Knutti (2018). Evaluating the accuracy of climate change pattern emulation for low warming targets. *Environmental Research Letters 13*, 055006. https://doi.org/10.1088/1748-9326/aabef2.

Tian, H., R. Xu, J. Canadell, and (2020). A comprehensive quantification of global nitrous oxide sources and sinks. *Nature 586*, 248–256. https://doi.org/10.1038/s41586-020-2780-0.

Trenberth, K., A. Dai, G. van der Schrier, P. D. Jones, J. Barichivich, K. R. Briffa, and J. Sheffield (2014). Global warming and changes in drought. *Nature Climate Change 4*, 17–22. https://doi.org/10.1038/nclimate2067.

Vitousek, S., P. Barnard, C. Fletcher, N. Frazer, L. Erikson, and C. D. Storlazzi (2017). Doubling of coastal flooding frequency within decades due to sea-level rise. *Scientific Reports 7*, https://doi.org/10.1038/s41598–017–01362–7.

Vousdoukas, M. I., L. Mentaschi, E. Voukouvalas, M. Verlaan, S. Jevrejeva, L. P. Jackson, and L. Feyen (2018). Global probabilistic projections of extreme sea levels show intensification of coastal flood hazard. *Nature Communications 9*, 2360. https://www.nature.com/articles/s41467-018-04692-w.

White, H. (1980). A heteroskedastic-consistent covariance matrix estimator and a direct test for heteroskedasticity. *Econometrica 48*, 817–838. https://doi.org/10.2307/1912934

Wigley, T. M. L. and S. C. B. Raper (1987). Thermal expansion of sea water associated with global warming. *Nature 330*, 127–131. https://doi.org/10.1038/330127a0.

APPENDIX 14A DATA

Both sets of SEM forecasts incorporate feedbacks from ocean warming and sea level rise and suggest an extrapolated transient climate response (TCR) (see also Schwartz, 2012) of about 2.3°C–2.5°C for a doubling of atmospheric CO_2 since the pre-industrial period. We calculate this range from the forecast increases of 42ppm CO_2 associated with a temperature increase of 0.37°C higher temperature after 20 years and 199ppm CO_2 associated with a temperature increase of 1.9°C after 90 years. These two forecasts entail ratios of 0.0088 and 0.0095°C/ppm respectively. A linear approximation to the transient climate sensitivity leads to a transient climate response – that is, the temperature response to a doubling of CO_2 concentrations from the pre-industrial level of 260ppm – of 2.3°C and 2.5°C using these ratios. We note that this is well within the 'very likely' (90% confidence) range of 1.3–3.1°C from the IPCC AR6.[7,8]

Table 14A.1 Data sources

CO_2	Atmospheric CO_2 in ppm, 1860–2018	NOAA then Mauna Loa since 1959
Temp	Global mean surface temperature deviations	1880–2021
OceanHeat	Ocean heat content deviations to 700 metres	1955–2019 also Levitus et al. (2009)
SeaLevel	Global sea level rise, 1881–2019	Church and White (2011), CSIRO 1880–2014

[7] The IPCC AR6 very likely equilibrium climate sensitivity (ECS) range, 2.1–7.7°, is both wider and centered on a much higher temperature, reflecting temperature adjustments to net heat flux stored in the deep ocean.

[8] Note that the doubling exercise associated with calculating TCR and ECS is distinct from the exercise of injecting CO_2 into the atmosphere, as recent studies such as those by Ricke and Caldeira (2014) and Dietz et al. (2021) have done. These instead rely on a linear relationship between temperature and cumulative CO_2 emissions following Matthews et al. (2009).